uc3m | Universidad Carlos III de Madrid

Bachelor's Degree in Biomedical Engineering

(2017-2018)

Bachelor Thesis

"Real-time EMG Control for Hand Exoskeletons"

Cristina Ibáñez Jiménez

Dolores Blanco Rojas

Luis Enrique Moreno Lorente

Leganés, 2018

ABSTRACT

The goal of this project is to develop a system for hand exoskeletons control in real time. Robotic systems are useful for rehabilitation therapies due to their ability to help patients perform repetitive movements. Hand recovery is especially critical because hands are necessary to perform many daily life activities. Exoskeletons developed for hand rehabilitation can benefit from a real-time control system that activates the robotic devices at the same time as the patient is performing a movement.

Real-time control of these systems can be achieved using different methods. In this project, electromyographic (EMG) signals from the patient's forearm are used. The controlled robotic systems are soft hand exoskeletons actuated with Shape-Memory Alloys (SMA) wires. The SMA wires are controlled with a microcontroller. The main objective of these exoskeletons is to help the patient with the movement of grasping an object and releasing it afterwards. Machine learning is used to detect the intention of the patient to grasp or release an object based on the patient's EMG signals. Once one of these movements is detected, real-time communication with the microcontroller is achieved and the necessary SMA wires are activated. The system is developed in Matlab, and it involves signal acquisition, signal rectification, signal segmentation, feature extraction, dimensionality reduction, signal classification, and communication with the microcontroller. To differentiate between the movements of grasping and releasing an object, three different classifiers will be tested: Artificial Neural Networks (ANN), Support Vector Machine (SVM) and K-Nearest Neighbors (KNN). Their performance will be compared using a confusion matrix and the best one will be selected for the system's algorithm.

Control is achieved with a time delay of less than 1 second for the action of grasping and of less than 2 seconds for the action of releasing is achieved, almost accomplishing the objective of developing a real-time control system. Several improvements are proposed to decrease this time delay.

Keywords: EMG, machine learning, control system, real-time, SMA wires.

AKNOWLEDGEMENTS

First of all, I would like to express my most sincere gratitude to Dolores Blanco Rojas, the director of this thesis, for giving me the opportunity to develop this project and guiding me through all the process. I would also like to thank Luis Enrique Moreno Lorente, for allowing me to work at his lab and for always having new suggestions to improve the project.

I also wish to express my thankfulness to Dorin Sabin Copaci and Álvaro Villoslada Peciña, doctorate students at the Robotics Lab, for always been keen to help me and for passing their enthusiasm and perspective on this field down to me.

Furthermore, I must thank Patricia Enríquez and Laura López, my colleagues, for allowing me to use their projects to test mine, and for creating such a great team work and collaborative environment.

Finally, I want to express my gratitude to my family and friends, who have been an inestimable support through the development of this thesis.

INDEX

GLOSSARY OF ACRONYMS

ACh Acetylcholine

ANN Artificial Neural Networks

AOTA American Occupation Therapy Association

AR Auto-Regressive

AUC Area Under the Curve

CE European Conformity

CNS Central Nervpus System

DOF Degree-Of-Freedom

EMG Electromyography

FDA Food and Drug Administration

FES Functional Electrical Stimulation

FMD Frequency Median

FMN Frequency Mean

FN False Negatives

FP False Positives

FR Frequency Ratio

HWARD Hand Wrist Assistive Rehabilitation Device

IMU Inertial Measurement Unit

KNN K-Nearest Neighbors

LDA Linear Discriminant Analysis

MAV Mean Absolute Value

MFMD Modified Frequency Median

MFMN Modified Frequency Mean

MUAP Motor Unit Action Potential

NMJ Neuromuscular Junction

PCA Principal Component Analysis

PSD Power Spectrum Density

PWM Pulse-Weight Modulator

QP Quadratic Problem

RMII Rutgers Master II

RMS Root Mean Square

ROC Receiver Operating Characteristic

SMA Shape-Memory Alloys

SSC Slope Sign Changes

SSI Simple Square Integral

STFT Short Time Fourier Transform

SVD Singular Value Decomposition

SVM Support Vector Machine

TIA Transient Ischemic Attack

TN True Negatives

TP True Positives

UC3M University Carlos III of Madrid

VR Virtual Reality

WAMP Wilson Amplitude

WHO World Health Organization

WL Waveform Length

WT Wavelet Transform

ZC Zero Crossing

INDEX OF FIGURES

INDEX OF TABLES

1. INTRODUCTION

1.1. MOTIVATION

Hand rehabilitation is necessary for patients whose hand motility has been reduced. Proper recovery is extremely important because hands are used for everyday activities such as eating, drinking, or bathing; essential for enjoying an independent life [1]. These actions fall under the category of Activities of Daily Living, according to the American Occupation Therapy Association (AOTA) [2]. In all those cases, the ability to grasp objects is required.

It has been reported that between 55% and 75% of stroke survivors continue to have limitations in upper-extremity functioning [3]. The recovery speed and success can increase with the use of robotic systems for rehabilitation, greatly improving the quality of life of these patients. However, these rehabilitation systems will only be practical if they are low cost, low weight, comfortable, easy to use, and have real-time control of the patient's and the system's motion.

This project will be focused on approaching the last key point. The ability to control robotic systems for rehabilitation using electromyogram (EMG) signals can provide many advantages over other control methods. A widely used control system is based on the measurements of force sensors. These devices are not ideal because they are dependent on changes in the patient's environment, while EMG sensors depend only on the patient's physiological changes. EMG offers also an advantage when using it for real-time motion control. EMG sensors can detect intentions of movement, therefore the control loop can start even before the patient starts moving.

1.2. OBJECTIVES

The main objective of this project is to develop a real-time control system for light-weight, low-cost hand exoskeletons. In order to test the control system, I will collaborate with Patricia Enríquez [4] and Laura López [5] , who are developing hand exoskeletons with different structures and materials and actuated with Shape-Memory Alloy (SMA) wires. The hand exoskeletons will help the patient with the movements of grasping and releasing a small object.

In order to achieve this objective, the system should be able to recognize the intention of the patient to grasp the object. At the time this recognition occurs, the system must

activate the SMA wires necessary for this movement so that they actuate the exoskeleton and help the patient with the action of grasping the object. Afterwards, the system should keep the SMA wires activated until the patient releases the object. When the system recognizes that the patient has released the object, it should inactivate the SMA wires used for the previous movement and activate the ones that open the exoskeletal hand. Ideally, the activation and deactivation of the actuators should occur at the same time as the patients grasps and releases the object.

1.3. STRUCTURE OF THE DOCUMENT

The thesis starts with an overview of the state of the art in Chapter 2. Firstly, the state of the art of hand rehabilitation therapies is reviewed (2.1). Afterwards, different robotic systems used for hand rehabilitation therapy are compared (2.2). Finally, the current applications of EMG signals for rehabilitation are analyzed (2.3).

Chapter 3 provides the physiological background of the generation of the EMG signals (3.1), and the technical aspects of the signal acquisition method (3.2).

Chapter 4 explains the methods used for signal processing, including signal rectification (4.1), signal segmentation (4.2), feature extraction (4.3), dimensionality reduction (4.4), and signal classification (4.5, 4.6). It also shows the results of using different methods for signal processing and classification, compares them and explains which will be the methods used in this project (4.7)

Chapters 5 explains in detail the communication between the computer and the actuators, and how the real-time control is achieved (5.1,5.2). Results from the control system are also presented in this chapter (5.3).

The socio-economic environment and the regulatory framework are reviewed in chapter 6.

Finally, chapter 7 provides a conclusion and states the future improvements that could be made to the project.

2. STATE OF THE ART

2.1. STATE OF THE ART OF HAND REHABILITATION THERAPIES

Hand motility reduction can have a variety of causes. Rehabilitation can benefit patients who have been affected by [6]:

- Vascular disorders, such as stroke, transient ischemic attack (TIA), subarachnoid hemorrhage, subdural hemorrhage and hematoma, and extradural hemorrhage.
- Infections, such as meningitis, encephalitis, polio and epidural abscess.
- Structural, trauma, or neuromuscular disorders, such as brain, head or spinal cord injury.
- Functional disorders, such as headache, seizure disorder, dizziness, and neuralgia. Patients with a functional movement disorder may experience symptoms such as tremors, jerks, twitches, spams or contractures [7].
- Degenerative disorders [7]:
    - Huntington's Disease, a progressive and degenerative disease caused by the deterioration of certain nerve cells in the brain.
    - Parkinson's disease, a progressive disorder caused by degeneration of nerve cells in the substantia nigra, which controls movement. Common symptoms include tremors, muscle rigidity or stiffness of the limbs.
    - Multiple sclerosis, an autoimmune disorder in which the immune system attacks the protective seath (myelin) that covers nerve fibers and causes communication problems between the brain and the rest of the body [8].

Neurophysiological problems resulting from these disorders include paralysis or problems with motor control. Most of the therapies used to help these patients are based on performing repetitive movements, which encourages brain plasticity and helps reducing disabilities. Hand rehabilitation therapies usually start with passive exercises, in which the therapists help the patients to move their muscles, and continue with active exercises, which involve physical effort from the patient [9].

Recently it has been emphasized the effectiveness of engaging in goal-directed activities, such as playing games, to promote coordination and increase patient's motivation [10]. Virtual reality (VR) systems have also been developed in order to encourage repetitive task practice. Virtual reality is a computer generated graphical environment that offers

opportunities for users to view and interact with the virtual environment in stereoscope. The introduction of haptic feedback can increase the sensory fidelity of VR [11]. Some advantages of this method include increasing the motivation of the patient, and the ability to automatically update task difficulty based on each user's progress [12]. There have also been identified some risks associated with VR such as eye strain, dizziness, and ataxia [11].

Another kind of therapy is mirror therapy. Although it was invented to alleviate the phantom limb pain, recently it has also been studied for hand motor function recovery [3]. It uses a mirror to create a reflective illusion of the affected limb in order to trick the brain into thinking that the movement has occurred without pain. The affected limb is placed behind the mirror, which is sited so the reflection of the opposing limb appears in place of the hidden limb. This approach exploits the brain's preference to prioritize visual feedback over somatosensory and proprioceptive feedback concerning limb position [13].

2.2. ROBOTIC SYSTEMS USED IN HAND REHABILITATION THERAPIES

Conventional therapies are costly and labor-intensive because they require manual interaction with physical therapists [14]. The use of robotic devices for rehabilitation therapies has increased due to their ability to perform repetitive tasks on patients. Furthermore, they can be used to quantitatively evaluate the patient's progress. Several comprehensive reviews on these robotic systems have been carried out [14]–[16]. Although all of these robotic systems share a common objective – to provide a training platform that can be used by patients to recover their hand motility and their ability to grasp objects in order to allow them to perform daily activities – these systems vary widely in terms of actuated degrees-of-freedom (DOFs), range of motion and design philosophy [17].

Most systems fall in the category of exoskeletons, since the robot joints are aligned with the anatomical joints. These devices are useful because they can provide direct control of these hand joints [17].

Hand exoskeletons vary on the number and the type of actuators they use. For example, Hand Exoskeleton Rehabilitation Robot (HEXORR) only uses two actuators, but is able to provide physiologically accurate grasping patterns. Other designs incorporate up to 18 actuators, hence, they can control more DOFs [17].

Regarding the type of actuators used by hand exoskeletons, we can distinguish three main tendencies:

- Electrical motors, used by HEXORR [17], Amadeo [15], Cable-Actuated Rehabilitation system (HandCARE) [18], Rutgers Master II (RMII) [19], Haptic Knob [20] and InMotion Hand Robot [21]
- Pneumatic actuators, used by Hand mentor [22], Robotic Assisted Upper Extremity Repetitive Therapy (RUPERT) [23] and Hand Wrist Assistive Rehabilitation Device (HWARD) [24]
- Passive actuators, present in Hand Spring Operated Movement Enhancer (HandSOME) [25]
- Functional Electrical Stilumation (FES), which uses the natural actuators of the body's muscles instead of external actuators. To achieve this, electrical stimulation is applied to the targeted muscles, leading to their contraction. FES significantly reduces the weight of the device [15]. Examples include NESS H200 [26], and the EXOSLIM device [27].

Exoskeletons using electrical motors make the machines large, heavy and costly, which is not the optimal situation for a clinical use and much less optimal for a home-care use [28]. Recently, there have been some advances in finding new kind of actuators. Shape Memory Alloys (SMA) are materials that have the ability to recover their original shape upon heating to a critical temperature [14]. They are also light and inexpensive, which makes them ideal for actuating exoskeletons.

Currently there are people in the Robotics Lab of the University Carlos III of Madrid (UC3M) developing light-weight hand exoskeletons using SMA actuators.

In the literature there are few wireless robotic systems, such as NESS H200 [26], and there is an increasing trend of combining these systems with interactive games (Hand mentor [22] , Amadeo [29], InMotion Hand Robot [21]).

2.3. EMG APPLICATIONS

Reliable motion control is a key issue for the correct functioning of an exoskeleton, and it should take into account the patient's motion. The sensing methods that hand exoskeletons incorporate for the purposes of controlling the device include force sensing, usually performed at the fingertip, motion sensing, which is obtained by measuring the

bending angle of the finger, and surface electromyogram (EMG) signals, among others. EMG signals of the forearm muscles have been proposed as a method to estimate the user's intention to move the hand and consequently trigger the open/close movement of the hand exoskeleton. Although this method proved to be effective, it can only be used for subjects with a coherent and relatively strong EMG signal, which might not be the case for most rehabilitation patients[30]. Other drawbacks of using EMG signals for motion control include the fact that not all muscles responsible for hand motion can be measured by surface EMG sensors, and, due to the high density of different muscles in the forearm, EMG signal separation is particularly relevant [31].

Most of the current hand exoskeletons that make use of the EMG signals generated from the patient's muscle to start the exoskeleton's movement initiate the movement when the EMG signal exceeds a certain threshold [32]–[36]. Others control the pinching force in a manner that is proportional to the amplitude of the EMG signal [37].

Machine learning can also be used to characterize EMG signals. Artificial Neural Networks (ANN), Fuzzy Systems, Probabilistic model algorithms, Metaheuristic and Swarm intelligence algorithms, and some hybrid algorithms are being used for this purpose. Literature results show that near perfect performance (between 95% and 98% rate of success) can be achieved when using the mentioned machine learning methods [38]. Machine learning has been used by some students at the Robotics Lab of the UC3M. In the Bachelor's Thesis of Irene Méndez Guerra: "Implementation of a Neural Network-Based Electromyographic system for a printed robotic hand", in 2016 [39], she used artificial neural networks to classify seven different gestures with an acquisition system consisting on four electrodes placed directly on the skin of the patient. The advantage of using skin electrodes is that their location can be chosen so that they record signals of targeted muscles involved in specific movements. The main drawback of surface electrodes is that they require skin preparation (hair removal and skin cleaning) to create a stable contact with low skin impedance. Furthermore, electrode placing must be done in an extremely careful way so that they are placed in the exact same position every session. If this is not done properly, the signals will be significantly different from session to session and the classification performance will decrease. These issues make the system not very practical for a clinical set up.

In the Bachelor Thesis of Alejandro Sánchez Anillo: “Matriz de Electrodos EMG para la detección de movimiento de la mano” in 2017 [40], he overcame most of the problems from Elena’s acquisition system by using Myo Armband, a bracelet developed by the company Thalamic Labs which consists on a wearable device that recognizes hand gestures in real-time using eight surface EMG sensors positioned on the forearm and an inertial measurement unit (IMU) containing an accelerometer and a gyroscope [41]. Using both the EMG signals and the gyroscope signals, Alejandro was able to differentiate between twelve hand gestures. This classification was done by obtaining the Mean Absolute Value (MAV) of the eight EMG signals and determining which muscles were involved in each gesture. For some hand movements, gyroscope data was also used for discrimination. The Myo Armband does not require skin preparation to work properly and it does not have to be placed exactly in the same position in every session to record similar signals from the same muscle.

3. EMG SIGNAL

3.1. PHYSIOLOGY

Electromyography is the recording of the electrical activity of muscle tissue, using electrodes attached to the skin or inserted into the muscle [42]. To understand the EMG signals, one must first understand how these bioelectrical signals are generated in the muscles.

In the nervous system, the somatic motor pathway (Figure 3.1) controls skeletal muscles. It has a single neuron that originates in the central nervous system (CNS), either in the brain or in the spinal cord, and projects its axon to the targeted skeletal muscle. The synapse of a somatic motor neuron on a muscle fiber is called the neuromuscular junction (NMJ) (Figure 3.2) [43].

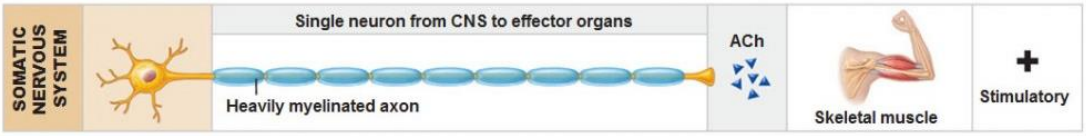

Figure 3.1 Somatic motor pathway [44]

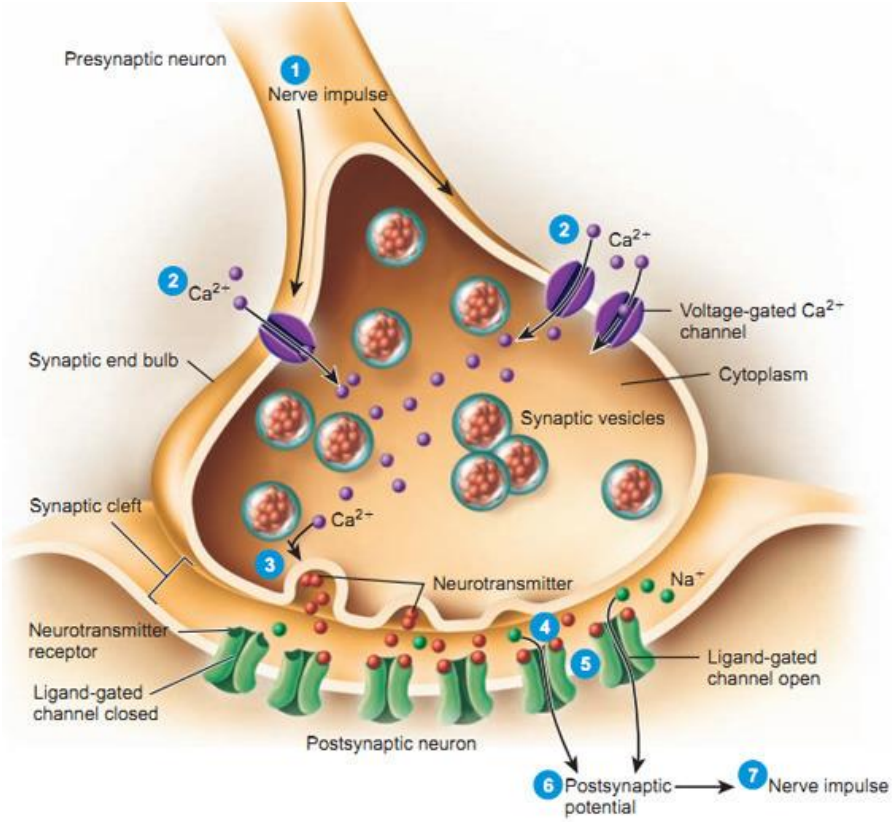

Figure 3.2 Neuromuscular junction [45]

As Figure 3.2 shows, nerve impulses arriving at the axon terminal open voltage-gated Ca^{2+} channels in the membrane. Calcium diffuses into the cell down its electrochemical gradient, triggering the release of a neurotransmitter, acetylcholine (ACh) contained in synaptic vesicles. Acetylcholine diffuses across the synaptic cleft and combine with neurotransmitter receptors on the skeletal muscle membrane [43]. The binding of the neurotransmitter to the receptor opens ligand-gated Na^{+} channels and Na^{+} enters the muscle cell, depolarizing it and generating a nerve impulse.

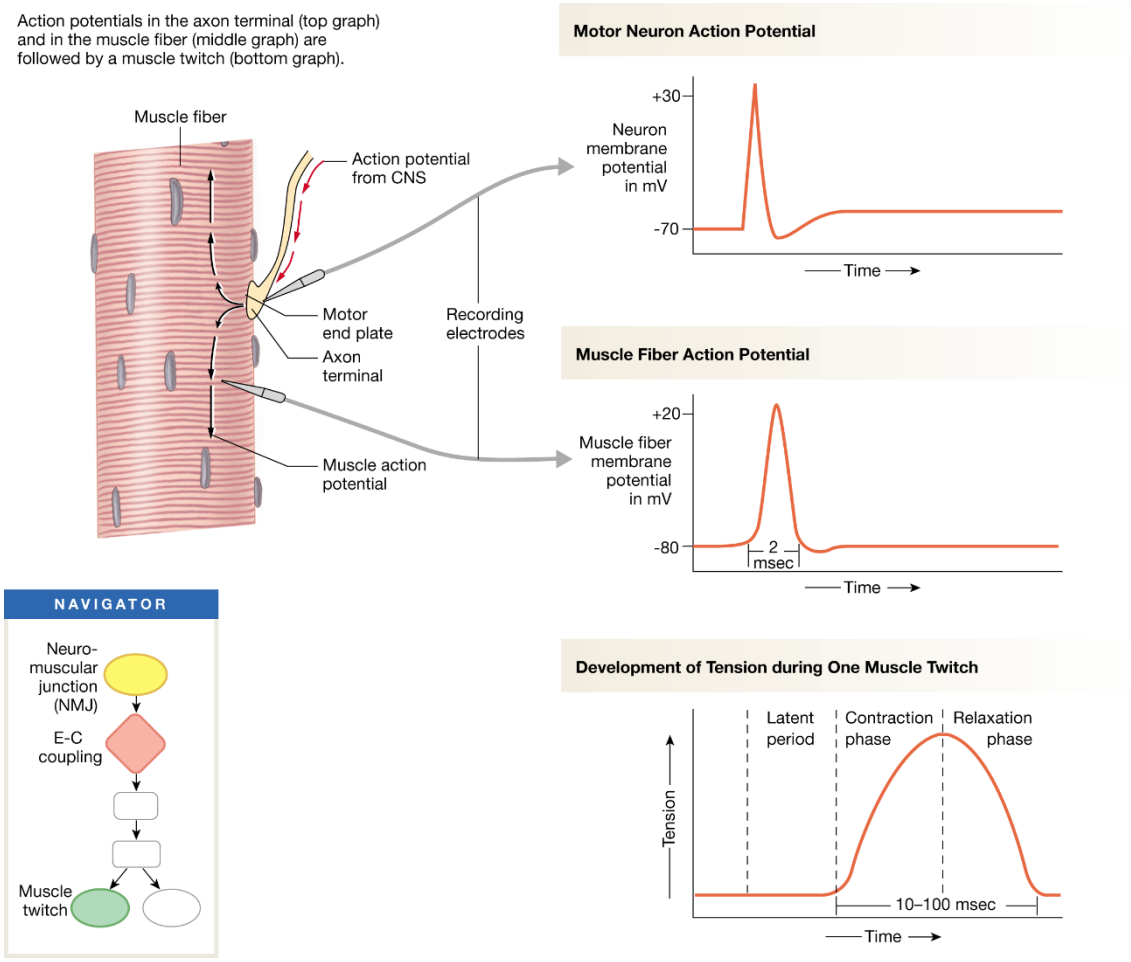

Figure 3.3 Timing of E-C coupling [43]

The somatic motor neuron action potential generates the skeletal muscle action potential, which is followed by muscle fiber contraction. This combination of electrical and mechanical events in a muscle fiber is called excitation-contraction coupling (Figure 3.3) [43]. A single relaxation-contraction cycle is referred to as a muscle twitch.

The membrane potential of a muscle cell at any time is a function of the net electrochemical gradients of ions that the membrane is permeable to at that time, and the permeability of the membrane depends on which ion channels are open. The resting

membrane potential in skeletal muscle cells goes from -70 to -90 mV. When Na^+ channels open and the muscle cell is depolarized, it reaches a potential of up to +30 mV [46].

Muscle fibers are not activated individually. Single motor neurons innervate multiple muscle fibers. The motor neuron and the muscle fibers it innervates are collectively called a motor unit. All of the muscle fibers in a motor unit are fired each time a motor unit fires. The number of muscle fibers within a motor unit varies within and between muscles. Small motor units are used for fine movements while large motor units are predominant in muscles used for gross vigorous movements [46]. The electrical activity recorded by EMG corresponds to the combination of the action potentials of all the muscle fibers present in the motor units activated when the patient voluntarily contracts the muscle [47]. This combination of action potentials is called the Motor Unit Action Potential (MUAP). The summation of electrical activity created by each active motor unit is the myoelectric signal[48]. Before amplification, EMG signal's range of amplitude is 0-10 mV (+5 to -5) with a frequency range of 10-500 Hz.

3.2. SIGNAL ACQUISITION

EMG signal is acquired non-invasively using a Myo™ Gesture Control Armband (Figure 3.4). Myo Armband, developed by Thalmic Labs, is a wearable device able to recognize hand gestures and control devices based on the recognized hand movements [49].

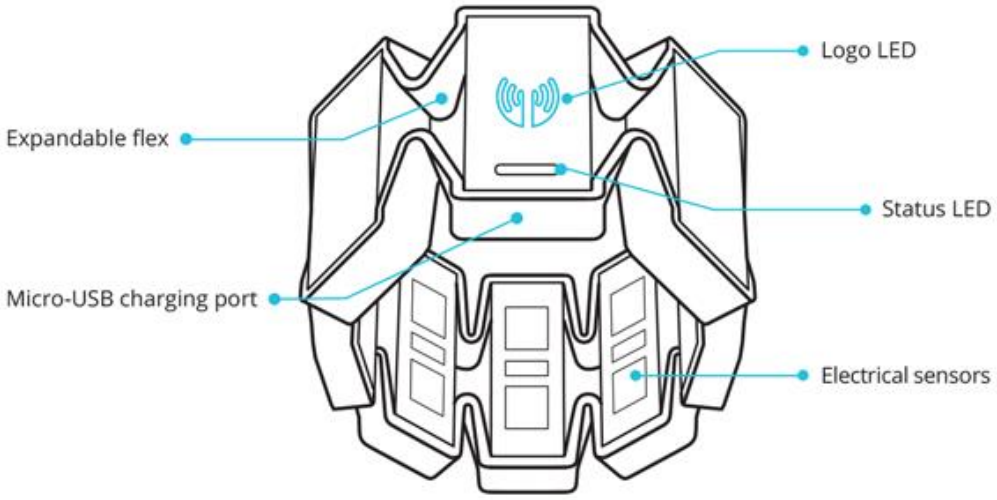

Figure 3.4 Myo Gesture Control Armband [50]

The device contains eight medical grade stainless still EMG sensors, and a highly sensitive nine-axis IMU, which includes a three-axis gyroscope, a three-axis

accelerometer, and a three-axis magnetometer [49]. Nevertheless, for this project, only the signals recorded by the eight EMG sensors will be used. The Myo Armband is connected to the computer using Bluetooth 4.0 Low Energy. Furthermore, it is stretchable, so it can comfortably fit each user's unique anatomy.

It has been shown that hand grip force is the result of forearm muscle activity [51], therefore, Myo should be placed in the proximal part of the forearm. It is convenient that the device is placed in the same position in every session in order to get optimal results. To do this, the logo LED is taken as a reference and it is placed right below the elbow, on top of the extensor and the flexor carpi (Figure 3.5), in the forearm, with the status LED pointing towards the hand (Figure 3.6).

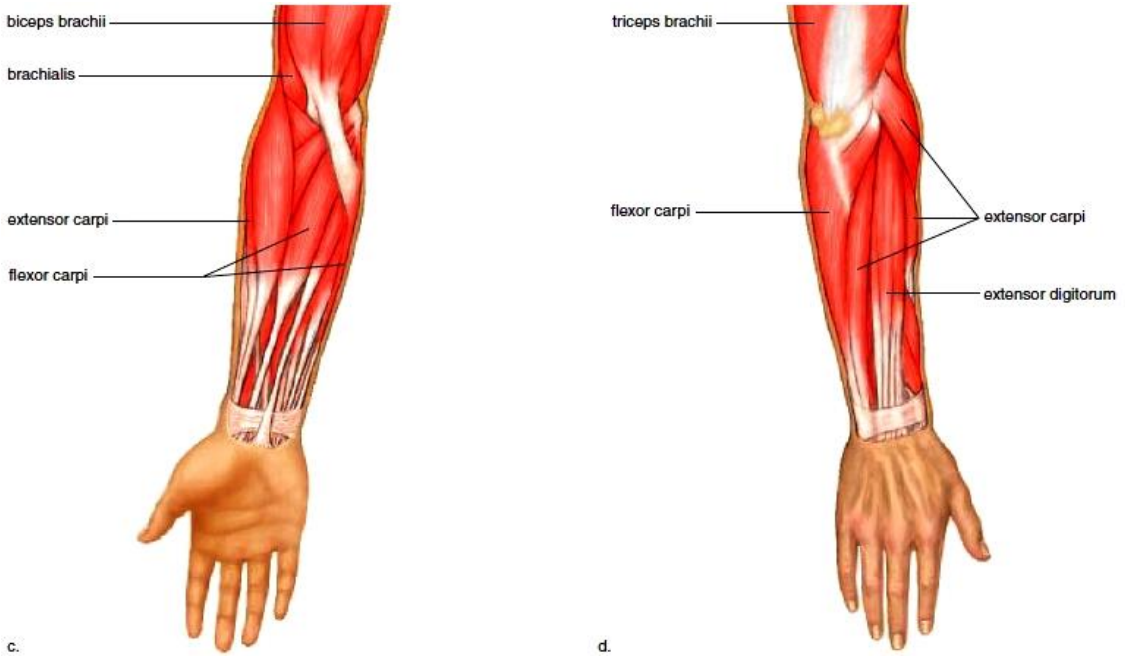

Figure 3.5 Muscles of the Forearm [52]

Figure 3.6 Myo Armband placed in the forearm

In order to be able to connect the Myo with a computer, the software Myo Connect and the SDK Myo SDK 0.9.0 must be installed in the computer [53]. The SDK takes care of all of the low level details related to Bluetooth connections and data transmission. The Bluetooth adapter must also be plugged into the computer. Most computers automatically detect the adapter and install the necessary drivers [54]. To turn on the Myo, it must be connected to the computer through a Standard Micro-USB Cable. The device can also be charged by plugging it to the computer (Figure 3.7).

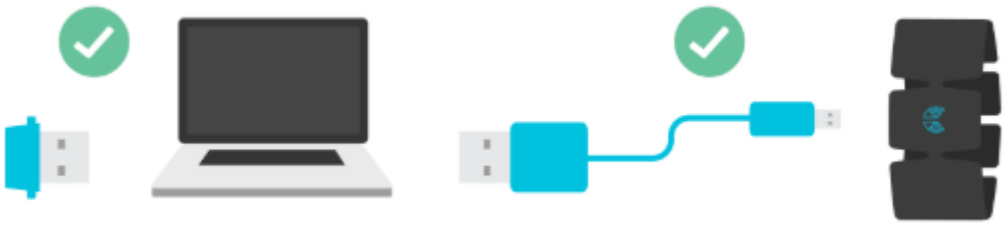

Figure 3.7 Bluetooth adapter and Myo Armband connected to the computer [55]

After placing the device in the forearm, it may need to warm up for a few minutes before it is able to work properly.

Myo SDK contains a library, `libmyo`, which allows applications with different programming languages to interact with the Myo Armband. In order to acquire the signals, the Myo SDK MATLAB MEX Wrapper, developed by Mark Tomaszewski, will be used. The package contains a simplified m-code class, MyoMex, that enables MATLAB users to stream data from one or two Myo devices at 50Hz (IMU and meta data) and 200Hz (EMG) [56]. The first step is to install MyoMex. This is done by typing: `>> install_myo_mex`. Secondly, a MyoMex instance must be built, by typing `>> build_myo_mex SDK_PATH`, where `SDK_PATH` is the location of the Myo SDK. After that, the objects of MyoData can be inspected. For this project, the objects used will be 'timeEMG', from which the number of samples stored in a given period of time can be obtained, and 'emg', which contains the values of the EMG signals from the eight channels (it is a matrix with eight columns) during the time elapsed from when the program starts to run to when the emg data is read. Therefore, the emg data accumulates in this variable until it is cleared. It is important to remember that the MyoMex instance should be cleaned before MyoMex is built another time.

A representation of the data acquisition process can be seen in the following diagram (Figure 3.8):

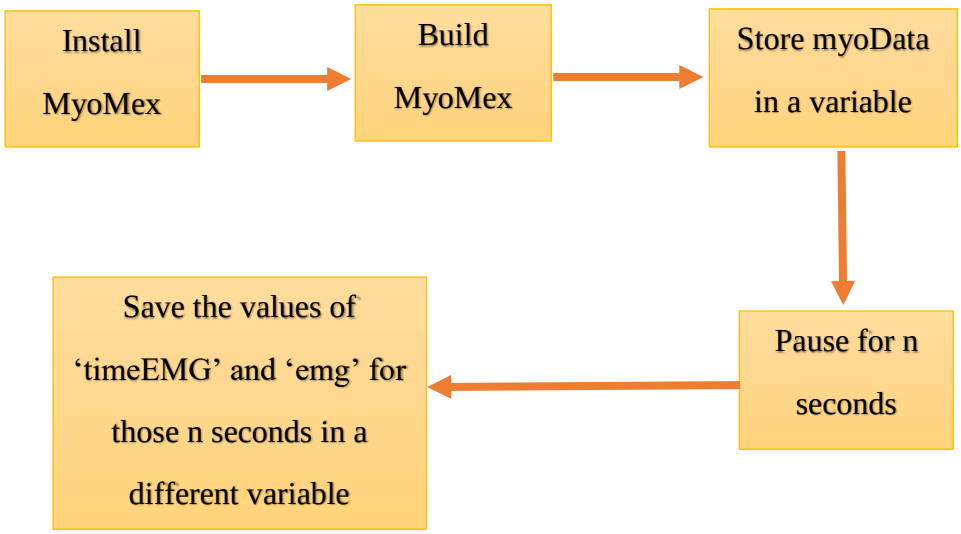

Figure 3.8 Data acquisition block diagram

The variable 'emg' is a matrix with eight columns, each corresponding to the signal recorded by each electrode in the Myo, and n rows, where n is the number of samples taken for a given time. Once this variable is saved, signal processing can start.

4. EMG SIGNAL PROCESSING AND CLASSIFICATION

4.1. SIGNAL RECTIFICATION

Rectification of the EMG signal involves taking the absolute value of the signal. This is useful because EMG signals show some symmetry with respect to the time-axis, so their mean value is always very close to zero. By taking the absolute value, the mean value of the rectified signal can be used as a feature for classification.

4.2. SIGNAL SEGMENTATION

Features are not obtained for the whole signal, but for signal segments. The length of the segments should not be either too short or too long. The first case can lead to bias and variance in feature estimation while the second case increases the computational load and the likelihood of failing to perform real-time operation [57]. The minimum interval between two distinct contractions is approximately 200 ms [58]. Therefore, a segment of data with a length of at least 200 ms contains enough information to estimate a motion state of the hand. Two methods can be used to segment the EMG signal: disjoint and overlapped segmentation (Figure 4.1).

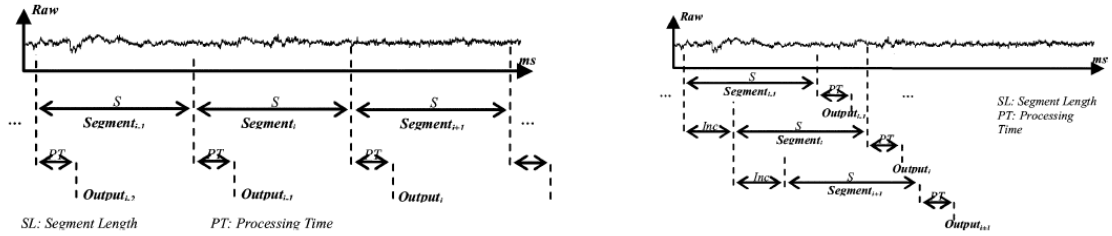

Figure 4.1 Disjoint (left) and overlapped (right) segmentation [57]

Oskoei performed an experiment in which he investigated the influence of segment length in classification using both segmentation methods [57]. The performance of classification in different segment lengths is illustrated in Figure 4.2. As can be seen in the figure, in segments with length longer than 300 ms, the accuracy of all features tested is high. Based on these results, the EMG signal is segmented in fragments of 300 ms. As MyoMex enables to stream EMG data at 200 Hz, segments of 60 samples are taken.

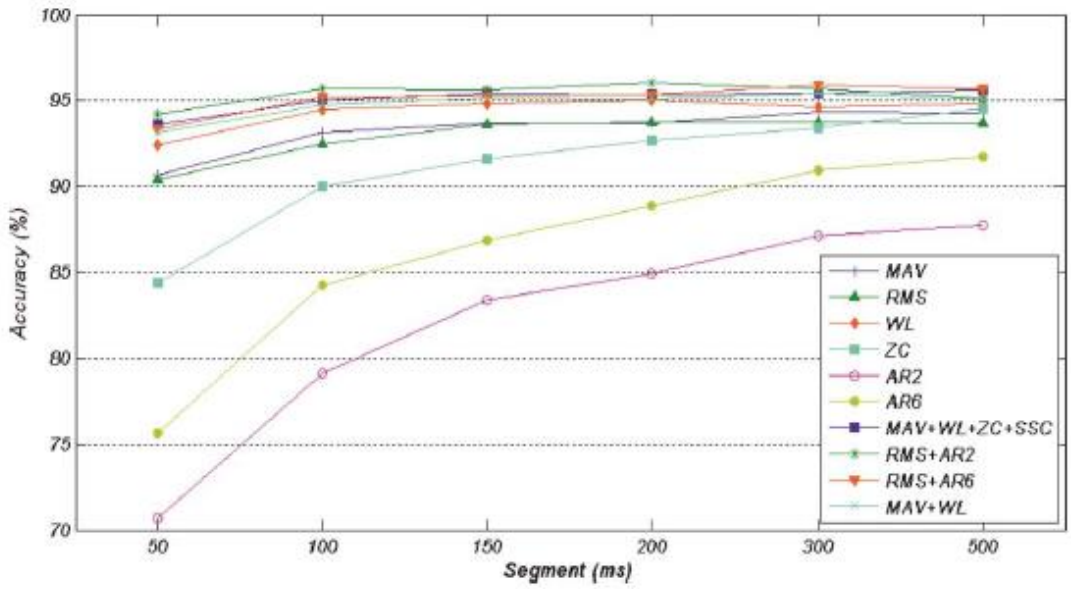

Figure 4.2 Dependance of classification accuracy on segment length [57]

Christodoulou et al. developed another method for signal segmentation in which the areas of low activity were eliminated [59]. This method is relevant for this project's purpose because both the grasping and relaxing signals have periods of time, especially at the beginning and at the end (Figure 4.3, Figure 4.4), where they are very similar, so those segments are not useful for classification. Based on this idea, a segmentation algorithm was developed in which only the most informative segment from each signal is taken. The segment is centered at the maximum value of the signal with a signal window of 60 samples. In this way, only the most discriminative part of the signal is used for classification.

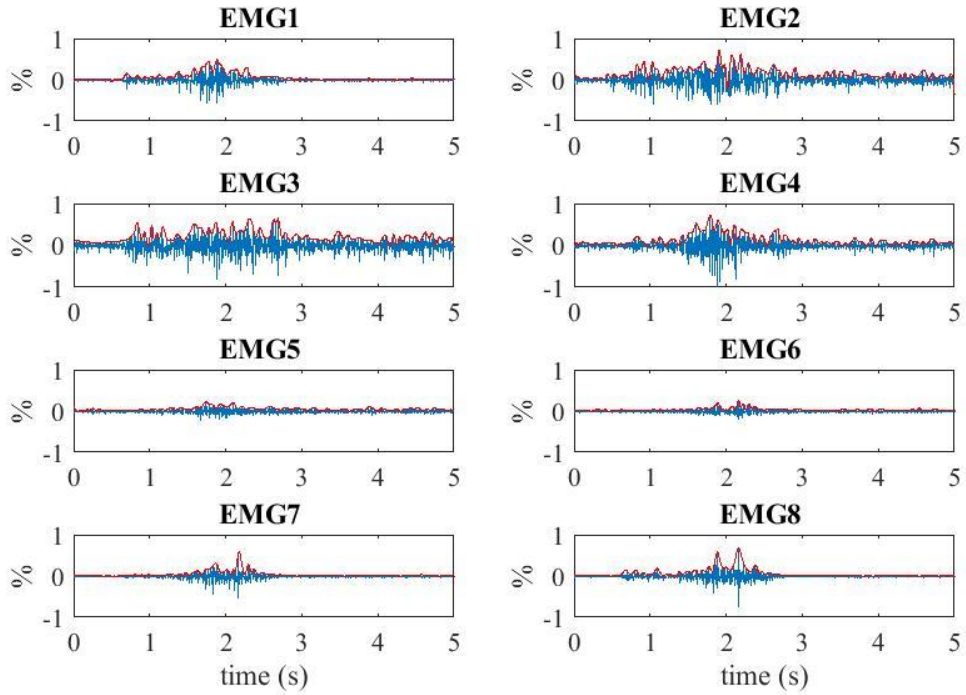

Figure 4.3 Scaled EMG signal values of the eight electrodes when the patient is grasping the object with respect to time (in s)

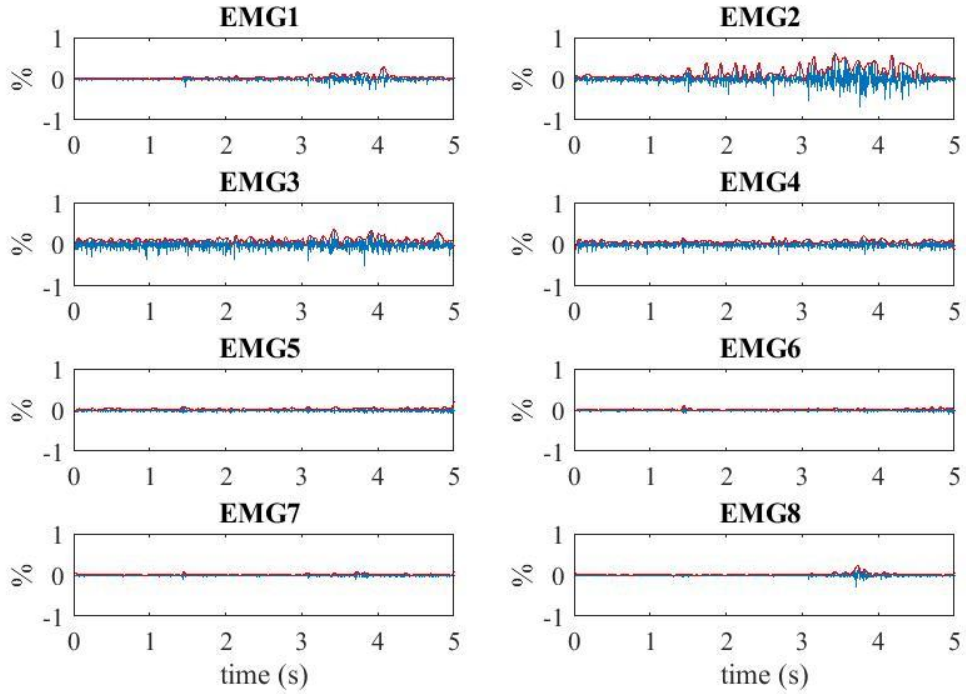

Figure 4.4 Scaled EMG signal values of the eight electrodes when the patient's hand is relaxed with respect to time (in s)

4.3. FEATURE EXTRACTION

Feature extraction involves the transformation of the signal into a set of features that can be used to feed the classifier. Classification will be more efficient than if than if the raw signal is used.

From an EMG signal there can be extracted different types of features:

1. Time domain features: They are widely used because their calculation is quick, as they do not require a transformation. They are computed based on the signal amplitude. Some examples of time domain features are stated in TABLE 4.1[60].

TABLE 4.1 EMG SIGNAL TIME DOMAIN FEATURES

Mean absolute value (MAV):	$MAV = \frac{1}{N}\sum_{k=1}^{N}\|x_k\|, for\ i = 1, \dots, I-1$
Root mean square (RMS)	$RMS_k = \sqrt{\frac{1}{N}\sum_{i=1}^{N} x_i^2}$
Simple Square Integral (SSI)	$SSI_k = \sum_{i=1}^{N}(\|x_i^2\|)$
Willson amplitude (WAMP)	$WAMP = \sum_{k=1}^{N} f(\|x_k - x_{k+1}\|)$
Variance of the EMG (VAR)	$VAR = \sigma^2 = \frac{1}{N-1}\sum_{k=1}^{N} x(k)^2$

Zero crossing (ZC)	$sgn(-x_k \times x_{k+1}) and\ (\lvert x_k - x_{k+1} \rvert \geq threshold)$ (The threshold is included to reduce noise)
Slope sign changes (SSC)	$(x_k - x_{k-1}) \times (x_k - x_{k+1}) \geq threshold$
Waveform length (WL)	$l_0 = \sum_{k=1}^{N} \lvert \Delta x_k \rvert$

2. Frequency domain features: They are based on signal's estimated power spectrum density (PSD). In comparison with time domain features they entail more computational cost. Some examples of frequency domain features can be found in TABLE 4.2 [61].

TABLE 4.2 EMG SIGNAL FREQUENCY DOMAIN FEATURES

Auto-Regressive coefficients (AR)	$x_k = -\sum_{i=1}^{N} a_i x_{k-i} + e_k$
Frequency Median (FMD)	$F_{MD} = \frac{1}{2}\sum_{i=1}^{M} PSD_i$
Frequency Mean (FMN)	$F_{MN} = \frac{\sum_{i=1}^{M} f_i PSD_i}{\sum_{i=1}^{M} PSD_i}$

Modified Frequency Median (MFMD)	$MFMD = \frac{1}{2}\sum_{j=1}^{M} A_j$
Modified Frequency Mean (MFMN)	$MFMN = \frac{\sum_{J=1}^{M} f_i A_i}{\sum_{J=1}^{M} A_i}$
Frequency Ratio (FR)	$FR_j = \frac{\lvert F(\cdot)\rvert_{jlowfreq}}{\lvert F(\cdot)\rvert_{jhighfreq}}$

3. Time-frequency domain features: They can localize the energy of the signal both in time and in frequency, allowing a more accurate description of the physical phenomenon. These features involve transformations that could be computationally heavy [61]. They are represented in TABLE 4.3.

TABLE 4.3 EMG SIGNAL TIME-FREQUENCY DOMAIN FEATURES

Short Time Fourier Transform (STFT)	$STFT_X(t,w) = \int W * (\tau - t)x(\tau)e^{-jw\tau}d\tau$
Wavelet Transform (WT)	$W_x(a,b) = \int x(t)(\frac{1}{\sqrt{a}})\,\Psi * (\frac{t-b}{a})\mathrm{dt}$

The main difference between the STFT and the WT is the way each of them divide the time-frequency plane (Figure 4.5). While the time and frequency resolution of STFT tiles are constant, the time and frequency resolution of the WT tiles vary, but the area of each tile remains the same [62] .

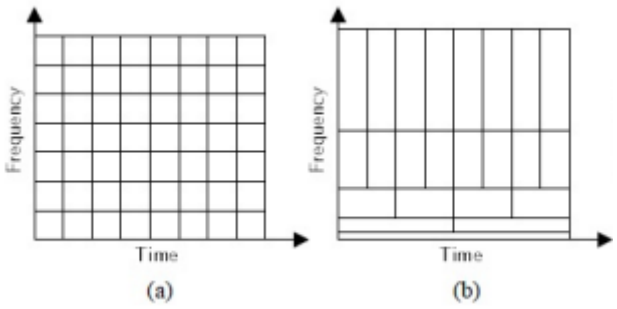

Figure 4.5 time-frequency plane of the STFT (a) and WT (b) [62]

4.4. DIMENSIONALITY REDUCTION

Dimensionality reduction is used to retain information that is important for class discrimination and discard that which is irrelevant. A classifier with fewer inputs has fewer adaptive parameters to be determined, leading to a classifier with better generalization properties According to Englehart et al. [63], there are two strategies to perform dimensionality reduction:

1. Feature selection methods, which attempt to determine the most informative subset of the original feature set. An example could be to select features using an Eucledian distance class separability (CS) criterion.
2. Feature projection methods, which attempt to determine the best combination of the existing features in order to create a more informative set. Examples of feature projection methods include Linear Discriminant Analysis (LDA) and Principal Component Analysis (PCA).

4.4.1. LINEAR DISCRIMINANT ANALYSIS (LDA)

LDA is a very common technique for dimensionality reduction. It is a supervised approach, meaning that it needs labeled data to work, and the probability distribution of the data has to be calculated. Although it is a well-used technique, it has some drawbacks. As an example, LDA fails to find the lower dimensional space if the dimensions are much higher than the number of samples in the data matrix. This is known as the small sample problem. It also fails if the classes are not linearly separable (linearity problem) [64].

To project the original data into a lower dimensional space, LDA performs three steps [64]:

1. Calculate the separability between different classes (i.e. the distance between the means of different classes), which is called the between-class variance or between-class matrix.
2. Calculate the distance between the mean and the samples of each class, which is called the within-class variance or within-class matrix.
3. Construct the lower dimensional space which maximizes the between-class variance and minimizes the within-class variance.

4.4.2. PRINCIPAL COMPONENT ANALYSIS (PCA)

PCA is an unsupervised method for dimensionality reduction. Its goal is to extract the relevant information from a data table, which represents observations described by several dependent variables, and to represent this data as a set of new orthogonal variables called principal components [65]. The principal components are actually the eigenvectors of the covariance matrix of the feature vector.

The 'pca' Matlab function [66] returns two matrices:

- The principal component coefficients: each column of the coefficient matrix contains coefficients for one principal component, and the columns are in descending order of component variance. By default, 'pca' centers the data and uses the singular value decomposition (SVD) algorithm. The coefficients are calculated with the training set of signals and saved in order to use them to reduce the dimensionality of a new feature vector. To obtain the new feature vector in the new dimensional space, it has to be multiplied by the coefficient matrix.
- The principal component score: the representations of the feature matrix in the principal component space. Rows of score correspond to observations, and columns correspond to components.

4.5. SIGNAL CLASSIFICATION

After extracting the features from the raw signal and obtaining a non-redundant set, the last step is to use a classifier. There are several algorithms to classify signals, and they can be divided into two big groups:

- Unsupervised methods: they do not require labeled data.
- Supervised methods: they require labeled data.

As the signals used in this project are labeled, meaning that it is known to which class they belong, only supervised classification algorithms will be reviewed and used.

4.5.1. ARTIFICIAL NEURAL NETWORK (ANN)

Artificial Neural Networks are based on the use of multitude of elemental nonlinear objects (artificial neurons) organized as networks, trying to imitate the way in which neurons are interconnected in the brain [62]. The response of these artificial neurons (Figure 4.6 (a)) is based on a weighted sum of its inputs: $net = \sum_{i=1}^{n} w_i x_i + w_{n+1}$, where x_i is the input of the neuron and w_i is the weight associated to x_i, which modulates the input signal.

The neuron output signal O is given by: $O = f(net) = \begin{cases} 1 & if\ w^T x \geqslant \theta \\ 0 & otherwise \end{cases}$ [67].

Where ɵ is the threshold element.

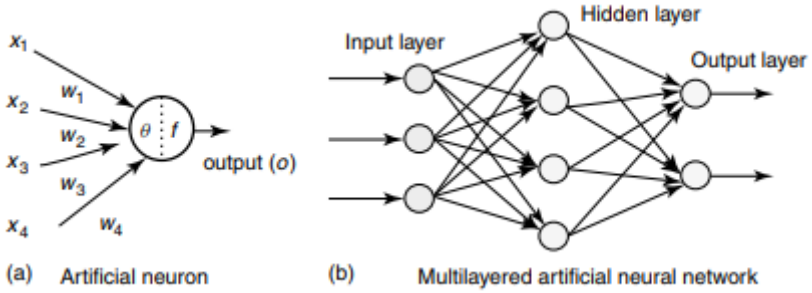

Figure 4.6 Architecture of an artificial neuron (a) and a multilayered neural network (b) [67]

The basic neural network architecture contains three types of neuron layers: input, hidden, and output layers (Figure 4.6 (b)). All the outputs of one layer are used as inputs for all neurons in the next layer. The weights can be set explicitly, using a priori knowledge, or the neural network can be trained by feeding it teaching patterns and letting it change its weights according to some learning rule. The network should not be overtrained. If this is the case, the network may become too adapted in learning the samples from the training set, and thus may be unable to accurately classify samples outside of the training set. The number of hidden neurons affects how well the network is able to separate the data. A large number of hidden neurons will give high performance in predicting training data but low performance on new data. With too few hidden neurons, the network may be unable to learn the relationships amongst the data. Therefore, selection of the number of hidden neurons is a crucial decision [67].

4.5.2. SUPPORT VECTOR MACHINE (SVM)

SVM is a popular tool to for machine learning tasks involving classification. It constructs an optimal separating hyperplane with the maximum margin between classes in a high-dimension feature space of training data that are mapped using a nonlinear kernel function (Figure 4.7). The kernel function transforms the original data space into a new space with a higher dimension. The data transformed into a higher dimension can be separated easily. This allows SVM to simulate nonlinear functional relationships [68]. Advantages of the SVM include relatively few free parameters to adjust, and the fact that the architecture does not have to be found via experimentation [57].

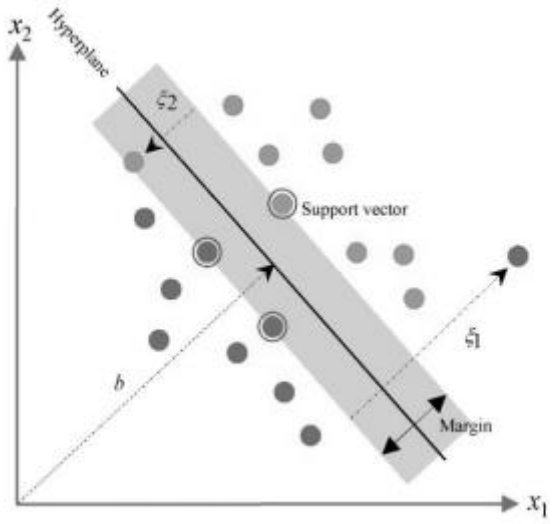

Figure 4.7 Support vector machine (SVM) to generalize the optimal separating hyperplane in linear separable data [68]

In SVM, training involves solving a quadratic programming (QP) problem. The solution to this QP problem is global and unique. To construct the optimal hyperplane with maximum-margin and bounded error in the training data (soft margin), one must solve the following QP problem:

$$min_{w,b}\frac{1}{2}\|w\|^2 + C\sum_{i=1}^{m}\xi_i$$

$$y_i(w \times \phi(x_i) + b) \geq 1 - \xi_i, i = 1, \ldots, m$$

The first term in this cost function maximizes the margin of separation between classes, and the second term provides an upper bound for the error in the training data [57].

This problem is solved using its Lagrange function. The solution shows that the optimal hyperplane, in feature space, can be written as a linear combination of the training samples. These informative samples, known as support vectors, construct the decision function of the classifier based on the kernel function. Different kernels can be selected depending on the data structure and type of the boundaries between classes: polynomial, sigmoid, etc [57].

Due to the way it is constructed, SVM is inherently a binary classifier, although there are some approaches to transform it into a multiclass classifier.

4.5.3. K NEAREST NEIGHBORS (KNN)

KNN utilizes a decision rule which assigns a class label to the input pattern based on the class labels represented by the K-closest neighbors of the vectors. It is commonly based on the Euclidean distance between a test sample and the training samples, although many other distance metrics can be used. A basic example for a 3-NN is shown in Figure 4.8. The nearest neighbors of point q1 are circle points, therefore q1 will be classified as the circle point's class. q2 has more cross points neighbors from its three nearest neighbors and therefore will be classified as the cross point's class [69].

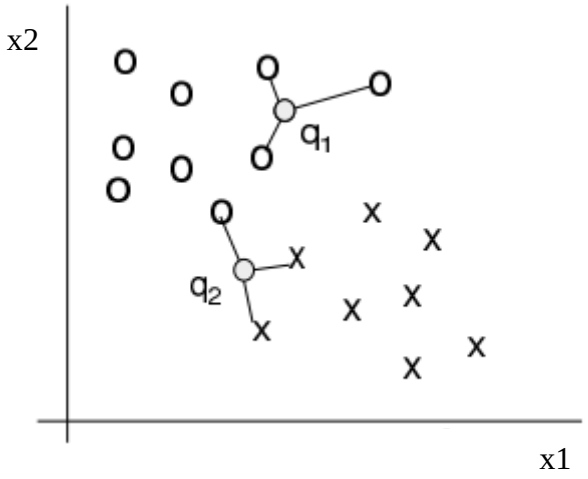

Figure 4.8 A simple example of 3-Nearest Neighbour Classification [69]

This method is popular due to its computational simplicity and its good results for many problems with small sample size. However, normally each of the sample vectors is considered equally important in the assignment of the class label to the input vector. This causes difficulty in places where the sample sets overlap. This problem is addressed by

assigning fuzzy class membership to the sample sets and thus producing a fuzzy classification rule. [70]

4.5.4. CLASSIFIER COMPARISON

The performance of the classifiers can be assessed using different measures. One of the most widely used is the area under the receiver operating characteristic (ROC) curve (AUC). [71] This measure is objective, as it requires no subjective input from the user. A perfect classifier will have an AUC of 1.

The correct and incorrect classification from each class is usually displayed as a confusion matrix (Figure 4.9). The row totals, CN and CP, are the number of truly negative and positive examples. The column totals, RN and RP, are the number of predicted negative and positive examples [71].

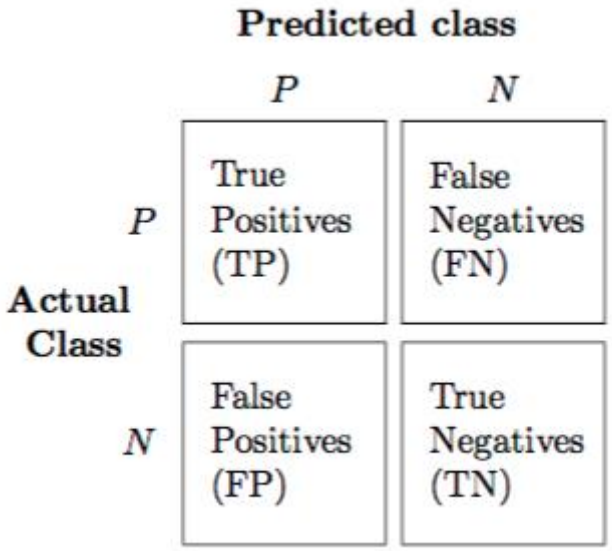

Figure 4.9 Confusion matrix [72]

From this matrix, meaningful measures can be extracted. The most typical one is accuracy, which is the ratio of the correct predictions over the total number of predictions. It measures the degree of veracity of a classification.

$$Accuracy\ (1 - Error) = \frac{TP + TN}{CP + CN}$$

Sensitivity is the proportion of true positives that are correctly classified. It shows how good the classifier is at identifying different classes.

$$Sensitivity = \frac{TP}{CP}$$

Specificity is the proportion of the true negatives. It suggests how good the test is at identifying normal (negative) condition.

$$Specificity = \frac{TN}{CN}$$

4.6. CLASSIFIER TRAINING AND TESTING DATA

Signals from two different classes were acquired using the Myo Armband. The two classes correspond to a person catching the object (Figure 4.10) and a person with his or her hand relaxed (Figure 4.11).

Figure 4.10 Class 1: Patient grasping the object

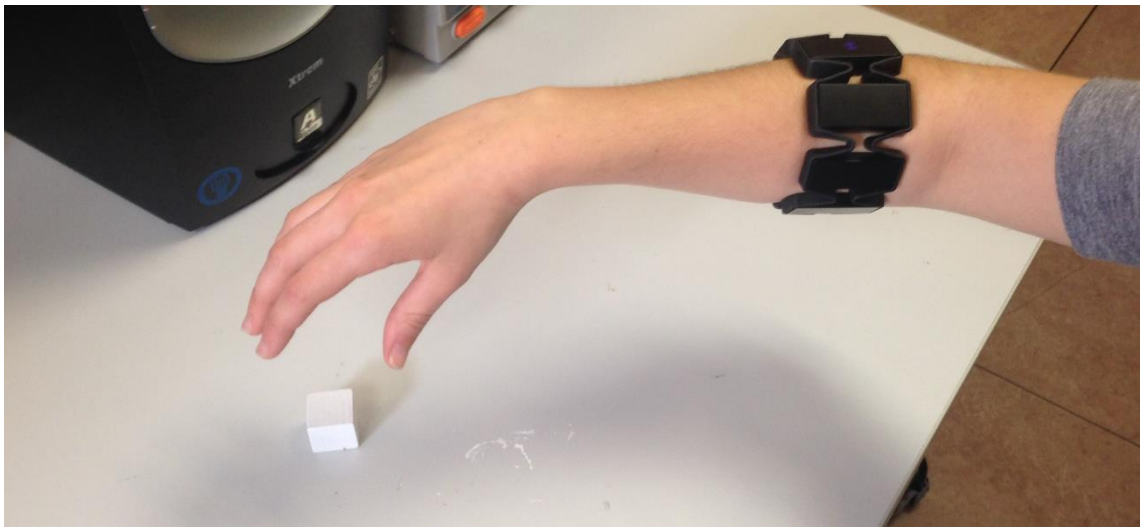

Figure 4.11 Class 2: Patient releasing the object

Eighty samples of one person catching the object were recorded and eighty samples of the same person's hand relaxed were recorded. Therefore, 160 samples were recorded in total. The samples were randomly divided into training and testing data as shown in TABLE 4.4.

TABLE 4.4 TRAINING AND TESTING SAMPLE DISTRIBUTION

	Training samples	Testing samples
Catching	60	20
Relaxing	60	20

4.7. RESULTS OF EMG SIGNAL PROCESSING AND CLASSIFICATION

Figure 4.12 shows that signal rectification provides data with an average less close to zero than if the absolute value is not taken. The mean value from all channels of the acquired EMG signal was -0.0072 while the mean value of the rectified EMG signal was 0.0498.

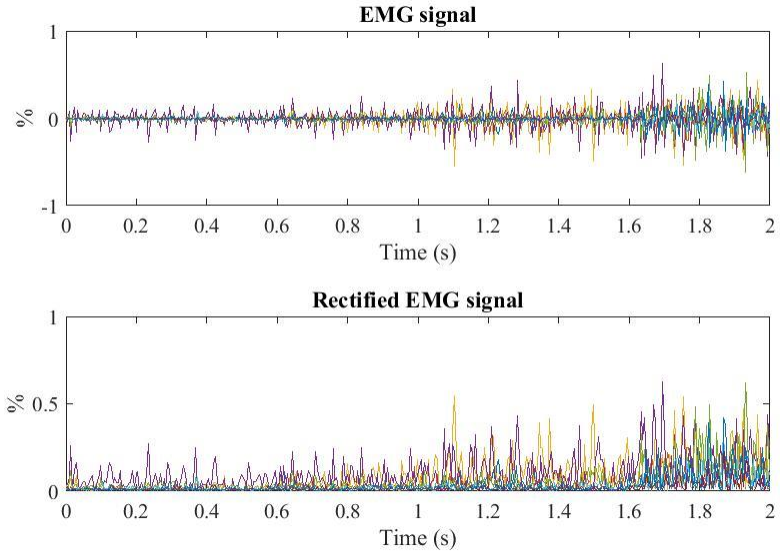

Figure 4.12 Acquired EMG signal (top) and rectified EMG signal (bottom) for the eight EMG channels

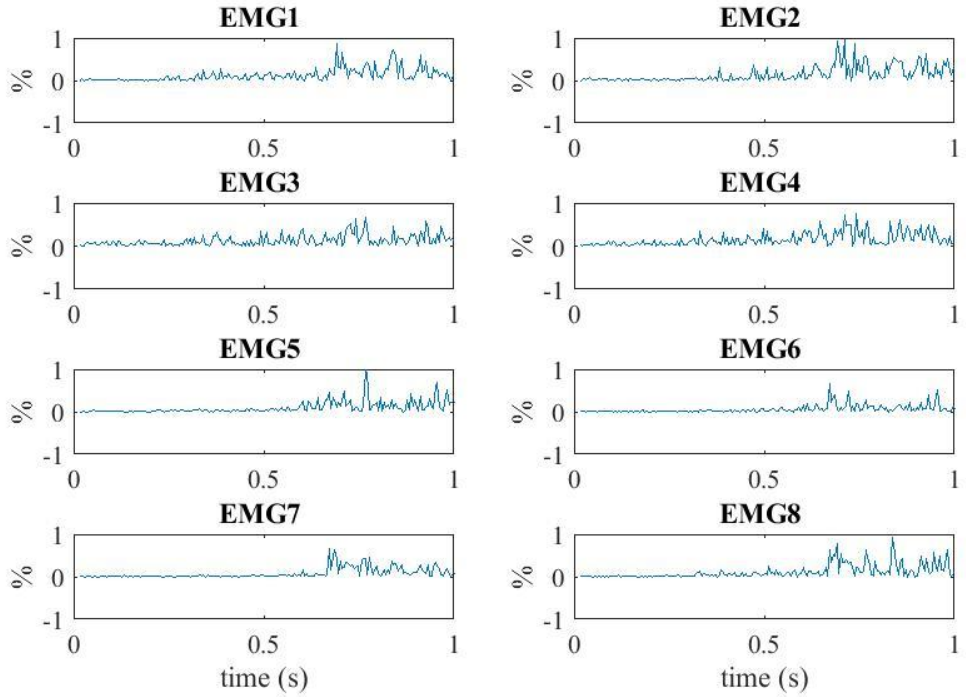

Figure 4.13 Rectified grasping scaled EMG signal for each channel with respect to time (in s)

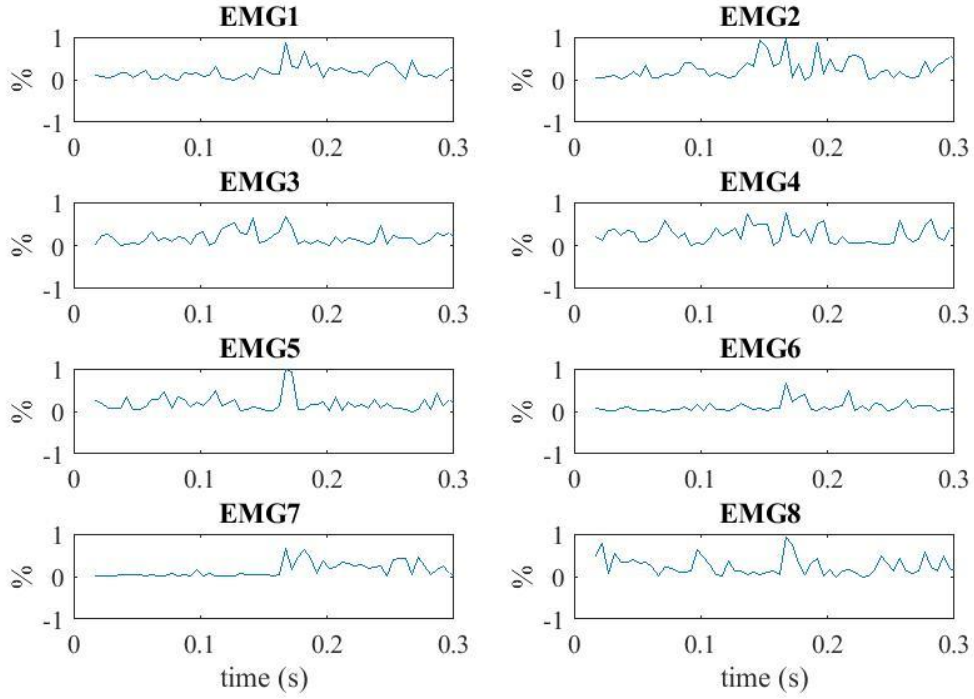

Figure 4.14 Rectified and segmented grasping EMG signal for each channel

The result of the signal segmentation can be seen in the comparison between the signal after rectification (Figure 4.13) and the rectified signal after segmentation (Figure 4.14). As the graphs show, the obtained segments are the most informative ones.

Due to their calculation simplicity and low computational cost, only the eight time domain features presented in TABLE 4.1 were used in this project. These features provide information regarding the amplitude of the signal.

The features obtain for one EMG recording are organized in a vector with 64 dimensions (eight features for each of the eight channels), as illustrated in TABLE 4.5.

TABLE 4.5 FEATURE VECTOR ORGANIZATION

Feature 1				**…**	**Feature 8**			
Channel 1	Channel 2	…	Channel 8	…	Channel 1	Channel 2	…	Channel 8

The features obtained for training and testing the classifier are organized in a matrix with each row representing a different observation.

The feature matrix is rescaled so that all features have values between -1 and +1. This is performed because if the value of one feature varies greatly, this feature can dominate over the rest and negatively influence the performance of the algorithm.

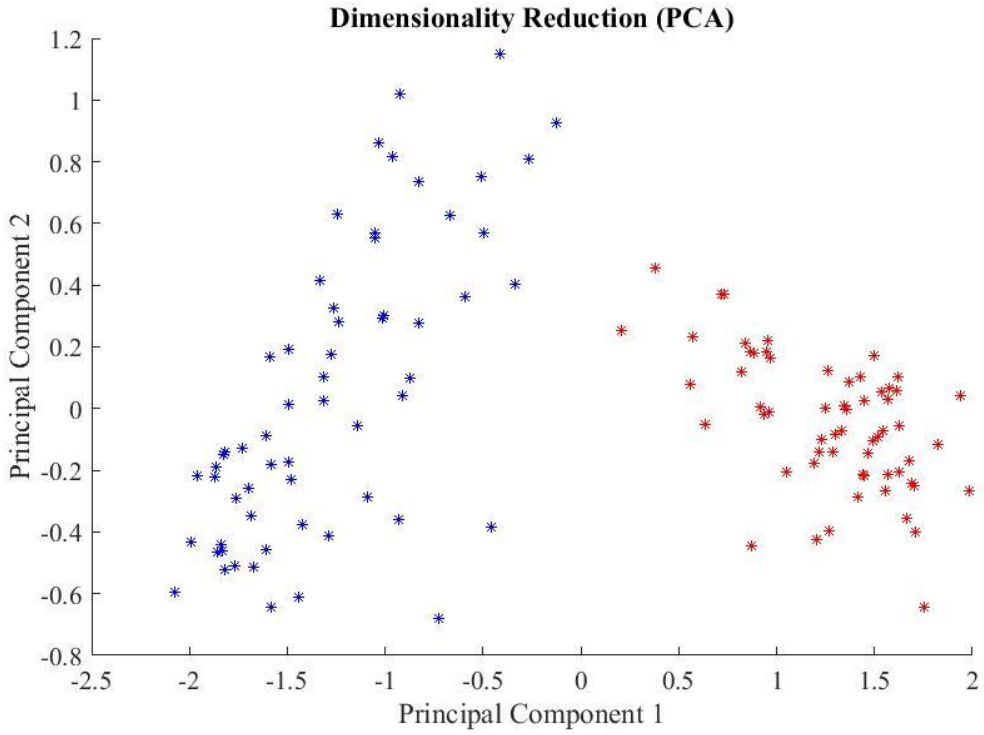

Figure 4.15 Two-Dimensional feature space using PCA

Figure 4.15 shows the training data distribution in a two-dimensional feature space generated using PCA. As can be seen, the two classes (signal of the patient grasping the object and signal of the patient's hand relaxed) can be well discriminated using the two principal components.

Three different classifiers were trained using this two-dimensional feature space:

SVM training:

Training of the SVM classifier was done using the Matlab function fitcsvm. The support vectors, plotted with the data in Figure 4.16, are the samples on the margin between both classes.

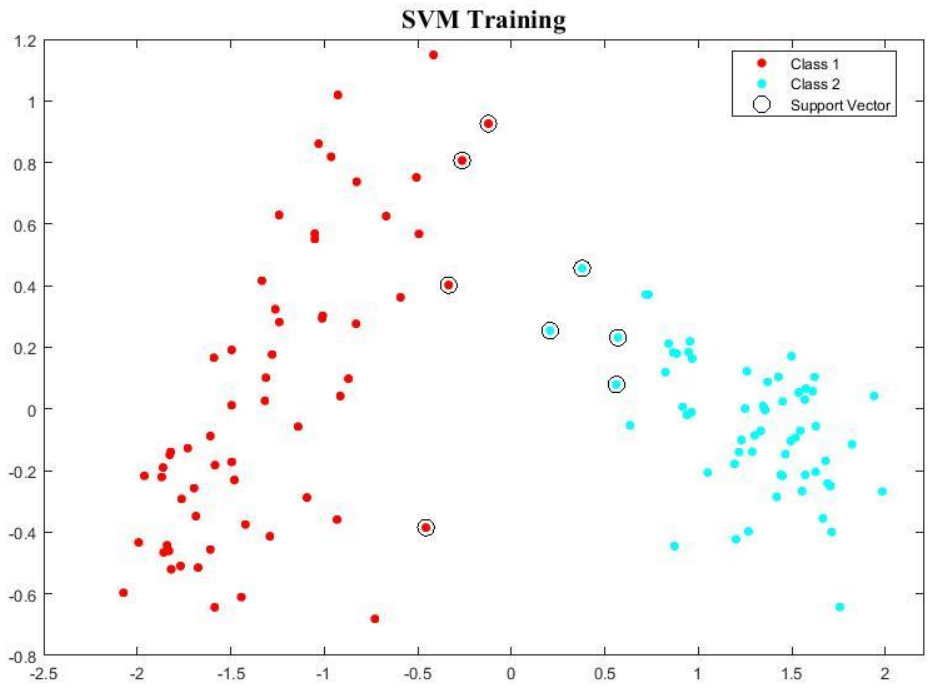

Figure 4.16 Plot of the data with the support vectors

Neural Network training:

A feedforward neural network was generated using the Matlab function `feedforwardnet`. In a feedforward neural network connections between neurons always go from a layer to the following one. The network was set to contain ten hidden layers. Training of the neural network was done using the Matlab function `train`. Figure 4.17 illustrates the training process of the neural network. The training set is divided randomly to validate

the performance of the classifier, which is evaluated using the Mean Square Error. Training is performed using the Levenberg-Marquardt algorithm, which minimizes nonlinear functions. Only eight iterations were necessary to achieve the minimum gradient. This can be explained by the size of the training set, which is not very big as it consists of 60 samples.

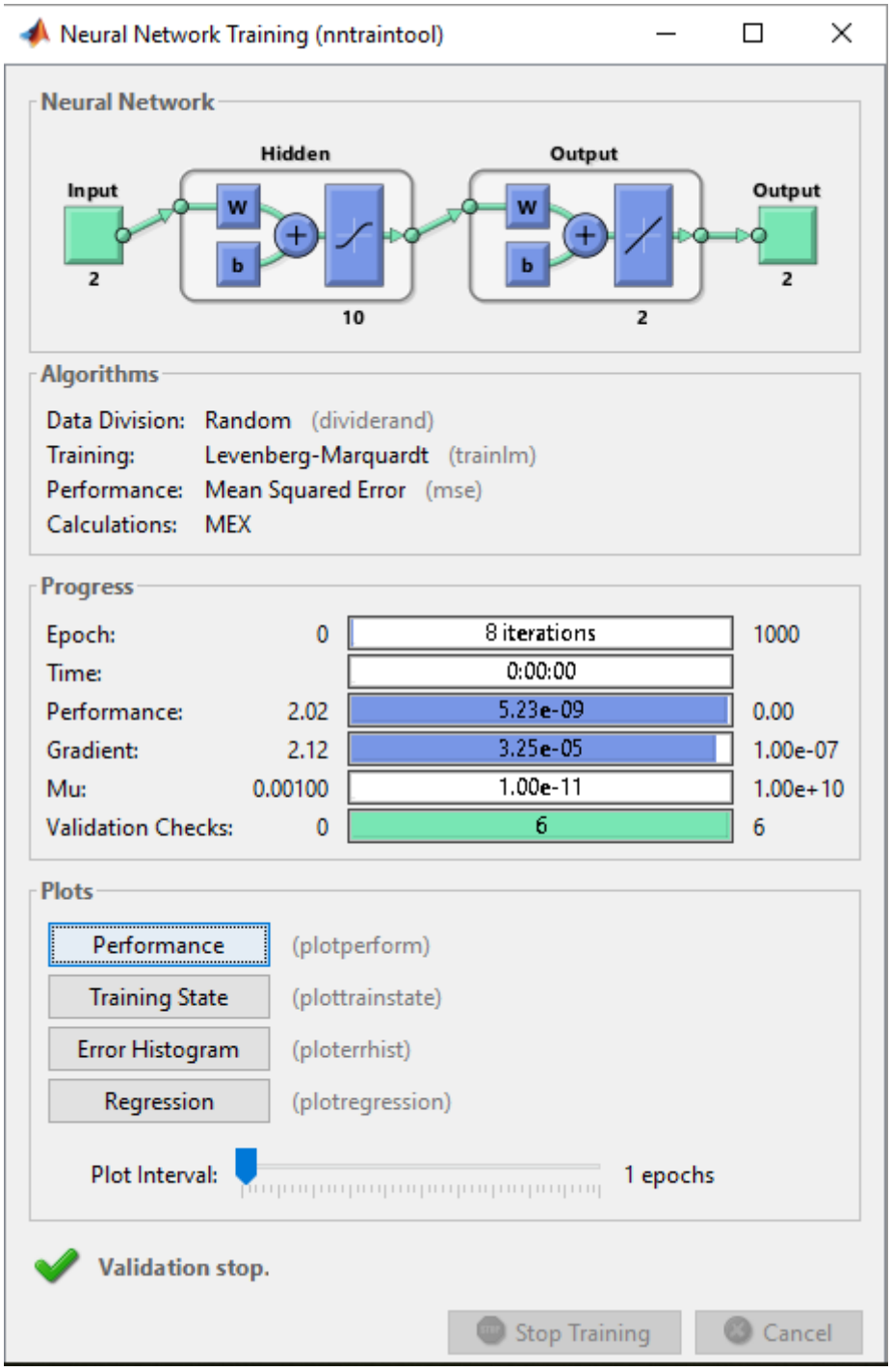

Figure 4.17 Neural Network training tool results

KNN training:

The KNN classifier was trained using the Matlab function `fitcknn`. The distance metric used was the Euclidean distance, and the number of neighbors used was 3.

Classifier comparison:

The confusion matrices from all classifiers were created using the testing data (TABLE 4.6, TABLE 4.7, TABLE 4.8).

TABLE 4.6 CONFUSION MATRIX FOR THE NEURAL NETWORK

	PREDICTED CLASS		
ACTUAL CLASS		CATCH	RELEASE
	CATCH	20	0
	RELEASE	2	18

TABLE 4.7 CONFUSION MATRIX FOR THE SVM

	PREDICTED CLASS		
ACTUAL CLASS		CATCH	RELEASE
	CATCH	20	0
	RELEASE	5	15

TABLE 4.8 CONFUSION MATRIX FOR THE KNN

	PREDICTED CLASS		
ACTUAL CLASS		CATCH	RELEASE
	CATCH	20	0
	RELEASE	3	17

Results show that all classifiers performed better when predicting that the patient was catching the object than when predicting the release of the object. This can be explained by the way in which the training data was acquired. The signals corresponding to the "releasing" movement were taken with the hand relaxed in different positions. Therefore, sometimes the algorithm will not detect that the patient has released the object until the hand is completely relaxed. The classifier with better performance was the Neural Network, with 95% of accuracy, as opposed to SVM, with 87.5% of accuracy, and KNN, with 92.5%. Therefore, the algorithm to activate and deactivate the SMA wires will use the trained neural network for classification.

Classifier performance was measured for three different subjects to determine if accuracy decreases when using the EMG signals from subjects whose signals were not used to train the neural network.

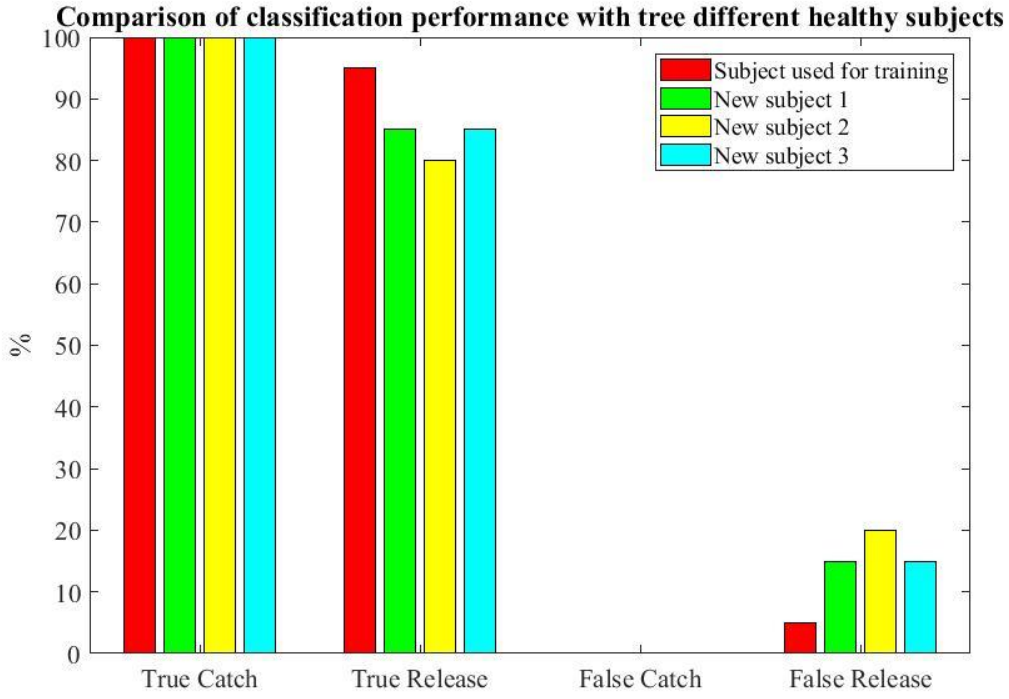

Figure 4.18 Classification performance with three different subjects

Figure 4.18 shows that for the action of catching the object, 100% of accuracy was achieved for all subjects. However, for the action of releasing, all subjects performed worse than the subject whose signals were used to train the classifier.

5. REAL-TIME EMG CONTROL OF ACTUATORS

The main objective of the project is to develop a system that can control SMA actuators. These actuators will be used to move exoskeletal hands developed in the Robotics Lab of the UC3M. The ultimate goal is to help rehabilitation patients grasping objects. The control system is based on the EMG signals acquired from the Myo Armband. After these signals are acquired, they are processed and classified using a neural network. Once the classifier detects that the patient wants to grasp or release an object, a control signal will be sent to the controller, and the controller will activate the SMA wires that are used for the corresponding movement and deactivate the SMA wires that are used for the opposite movement. The hand exoskeletons developed by Patricia Enríquez [4] and Laura López [5] in their Bachelor Thesis use six different SMA wires, and use some of them for grasping the object and some of them for releasing it. At the beginning all wires are deactivated, so the first time that the patient grasps the object, only the wires used for grasping are activated. When the system stops, all wires are deactivated. A scheme of the grasping process is illustrated in Figure 5.1. A scheme of the releasing process is illustrated in Figure 5.2.

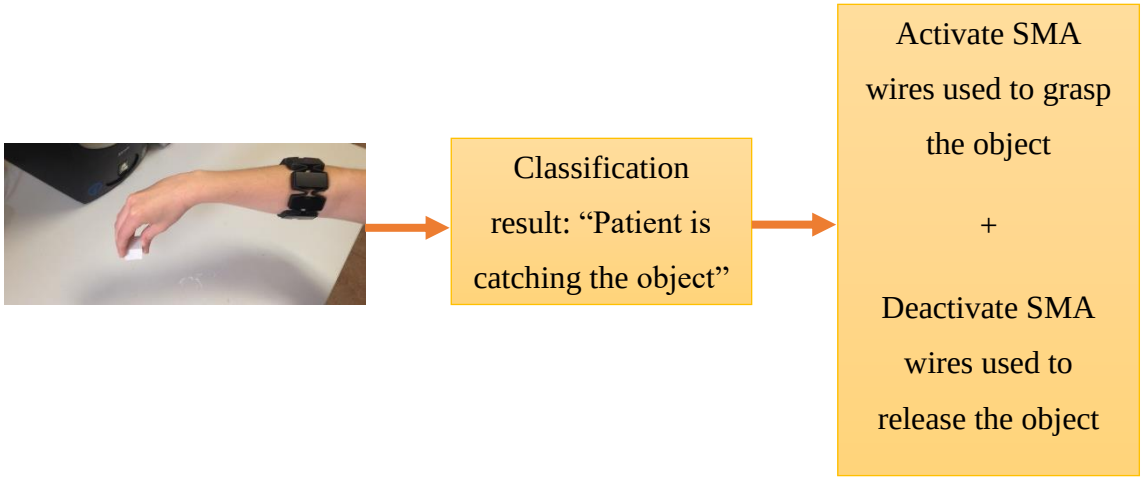

Figure 5.1 Scheme of the grasping process

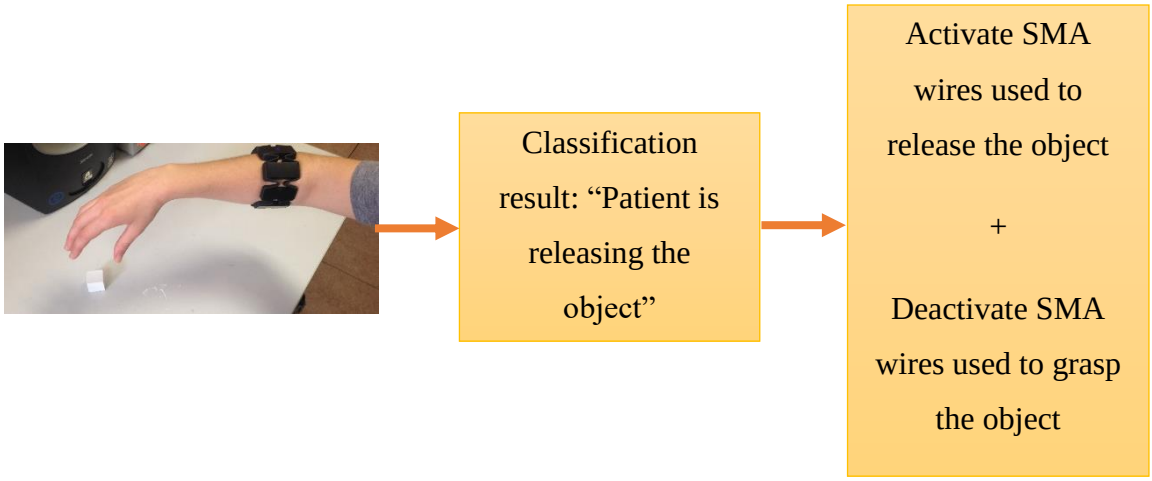

Figure 5.2 Scheme of the releasing process

5.1. SIMULINK MODEL TO CONTROL SMA WIRES

In order to understand how a Simulink Model can control SMA wires, the way in which SMA wires actuate the hand exoskeletons must be explained. As stated in the state of the art, SMA are materials that have the ability to recover their original shape upon heating to a critical temperature. The wires used in the Robotics Lab contract when they are heated. In order to heat the wires, current is applied to them. The microcontroller modulates the current that must be applied by using potentiometers that detect how much distance the wires have been contracted.

Two Simulink programs are used to control the SMA actuators: Bilineal_Simple and Bilineal_simple_HOST. They were developed to control a wearable elbow exoskeleton actuated with Shape Memory Alloy [73]. The sensor reading of these programs has been slightly modified because the sensor in the elbow exoskeleton was an absolute rotary encoder while the sensors used in the hand exoskeletons are potentiometers.

Bilineal_simple is the model that must be built into the microcontroller that controls the SMA wires. The variables used by the model include:

- MEDIDA_REAL, which is the measurement obtained from the potentiometers.
- PWM_PERCENT, which is the output of the PID controller.
- ERROR, which is the difference between the desired position of the wires and their actual position.

- ENABLE_CONTROL, which is a binary variable controlled by the user that can be either 0, if the control of the actuators by the model is not enabled, or 1, if the control is enabled.
- Position_Ref, which is the desired position of the wires specified by the user.

All these variables are stored six times, one for each of the six SMA actuators.

The model includes four main blocks: USB receiver, control logic, PWM output and USB send.

The USB receiver receives the ENABLE_CONTROL and Position_Ref data from the computer.

The control logic determines how the system responds to events or conditional changes, according to the PID shown in Figure 5.3. It also contains a sensor block which acquires the real measure from the potentiometers in the MEDIDA_REAL variable. After the actuators move, the control system receives the change in their position and adjusts them.

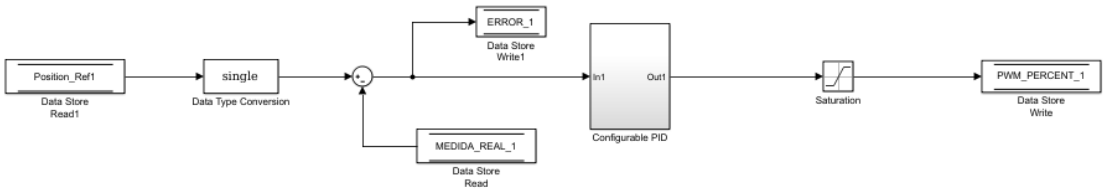

Figure 5.3 PID and bilineal term of control logic

The proportional, integral and derivative parameters can be modified to change the response of the system.

The pulse-weight modulator (PWM), generates an analog signal from a digital source. It multiplies the PWM_PERCENT variable, which is the output of the PID, with the ENABLE variable. Therefore, the PWM_PERCENT correction is only made if the ENABLE variable is 1.

The USB send sends the variables MEDIDA_REAL, PWM_PERCENT, and ERROR, back to the computer.

Bilineal_simple_HOST is a program used to visualize the data coming from Bilineal_simple, and change the parameters sent from the computer to Bilineal_simple.

The parameters that can be visualized are the same ones as the ones sent from the model to the computer: MEDIDA_REAL, PWM_PERCENT, and ERROR.

The parameters that can be changed are the ones that are sent from the computer to the model: ENABLE_CONTROL and Position_Ref.

5.2. COMMUNICATION MODEL TO ACHIEVE REAL-TIME CONTROL

Real time control of the actuators is achieved by instantaneously sending information from the computer to the microcontroller when the computer detects a movement. This is done using a Matlab function developed using the "Serial Communication in Matlab tutorial" from Esposito [74].

Before running the function, the program Bilineal_Simple, which is used to control the wires, must be built into the microcontroller. The microcontroller connects to the computer through a Serial Port. The first thing that must be done is to find the COM Port number that the device is using. Matlab uses a special variable type to keep track of serial connections: the Serial Object. The port number can be obtained automatically by trying to create a Serial Object without a port and catching the last error message. Once the Port Number is known, the real Serial Object can be created. In order to use the serial port object, it must be opened, and when it is not used, it can be closed. After opening the serial port, the values that need to be sent to the microcontroller (ENABLE_CONTROL and Position_Ref) are written, and data from the microcontroller is read. This communication is fast, so as soon as the Matlab program detects an action from the patient, it writes the new variables in the Serial Objects. The block diagram of the algorithm is illustrated in Figure 5.4.

The system starts recording 1 second of data. This data is processed and classified. If the classification output is that the patient's hand is relaxed, it records another second of data and processes and classifies it again. This happens until the classification output corresponds to the patient grasping the object. When this occurs, the program writes two variables in the microcontroller: ENABLE_CONTROL and Position_Ref. The ENABLE_CONTROL value sent is 1, to enable the control of the wires. Position_Ref is a vector [p1,p2,p3,p4,p5,p6]. Each value corresponds to the desired movement distance in mm of each of the six SMA wires connected to the microcontroller. The position values of the SMAs used for grasping and for releasing can be changed by the user. Due to the length of the wires used, the maximum distance that they can contract is 60 mm.

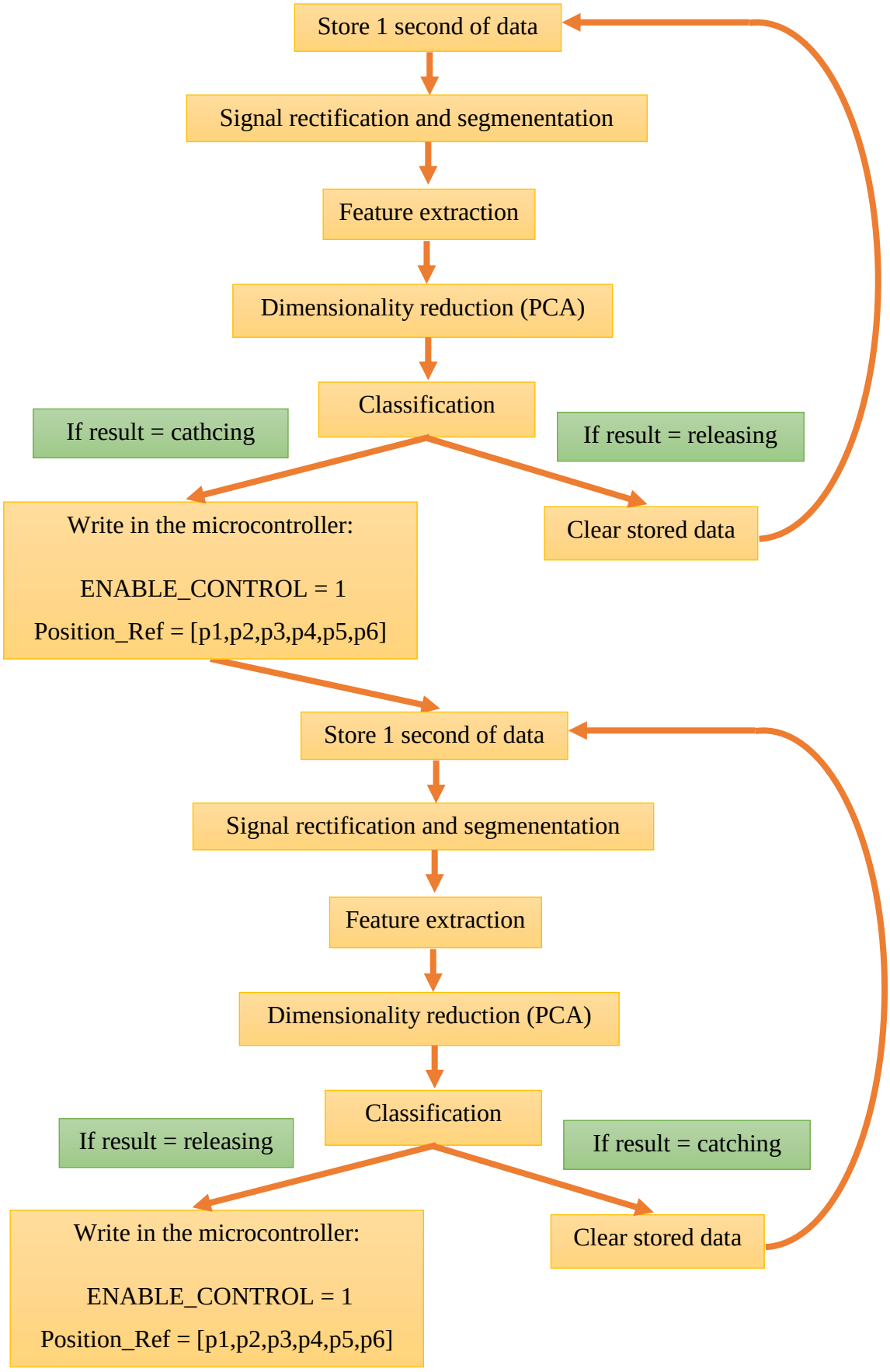

Figure 5.4 Block diagram of the real-time EMG control of the hand exoskeletons

For safety reasons, the program only allows to decide a reference position between 0 and 50 mm. The value of this distance depends on the force that is needed to move the exoskeleton. Usually closing the hand requires more contraction force than opening it. All the values of the wires that are not used are set to zero. Once these values are written in the microcontroller they do not change until the next values are sent. Therefore, the wires will remain in their reference position until another movement is detected or until the program stops.

After grasping, the system repeats the process of recording, processing and classifying 1 second of data until the classification output corresponds to the patient's hand relaxing. When this happens, the same data as before is sent, with a different Position_Ref vector. Now the values from the SMAs used for opening the hand are changed and the values from all other SMAs are set to zero. This process is repeated until the user decides that no more repetitions are needed.

To make the program user-friendly, a user interface (UI) was developed (Figure 5.5). The desired positions in mm of all the SMAs from each of the two movements can be easily changed by the user. After these positions are changed, the user just have to push the START button at the top-left part of the GUI and the program will start running. The plots will show the current EMG signals of the patient from each of the eight sensors. The text box will say 'CATCHING' when the program detects that the patient has catch the object (Figure 5.6) and 'RELEASING' when the program detects that the patient has released the object (Figure 5.7). The process of detecting that the patient is catching and releasing the object will continue until the user changes the drop-down button "Continue" from "YES" to "NO" (Figure 5.8).

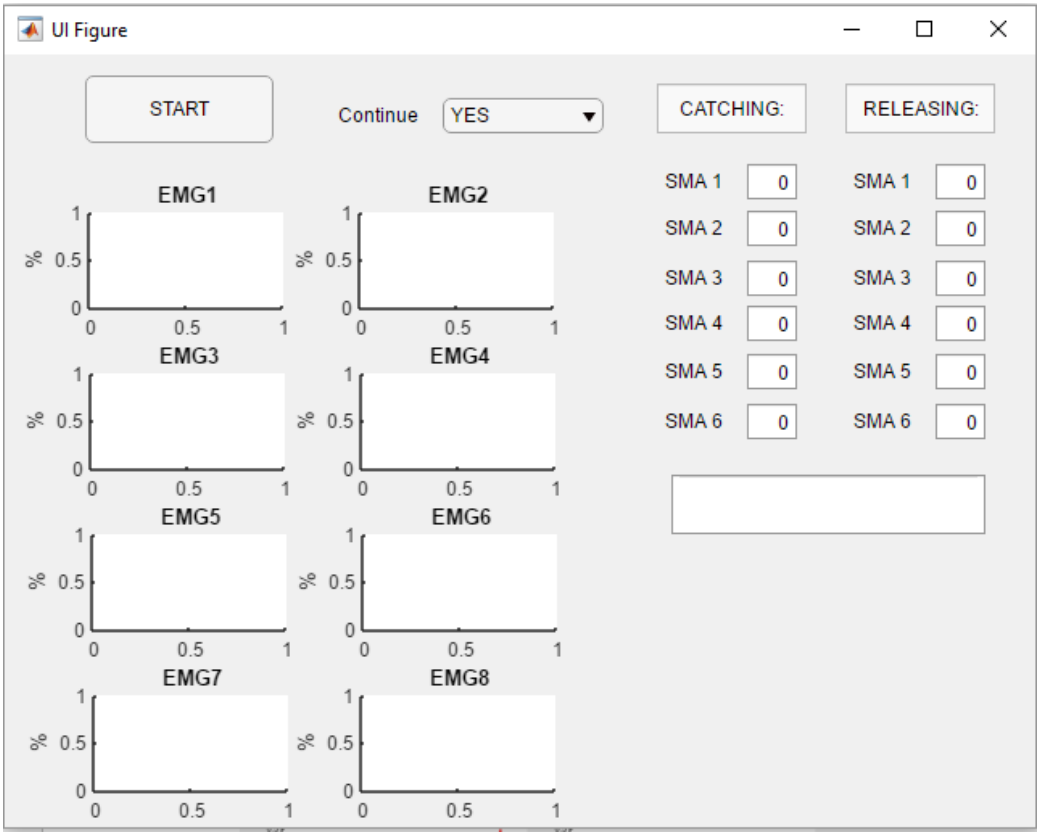

Figure 5.5 UI before the program starts

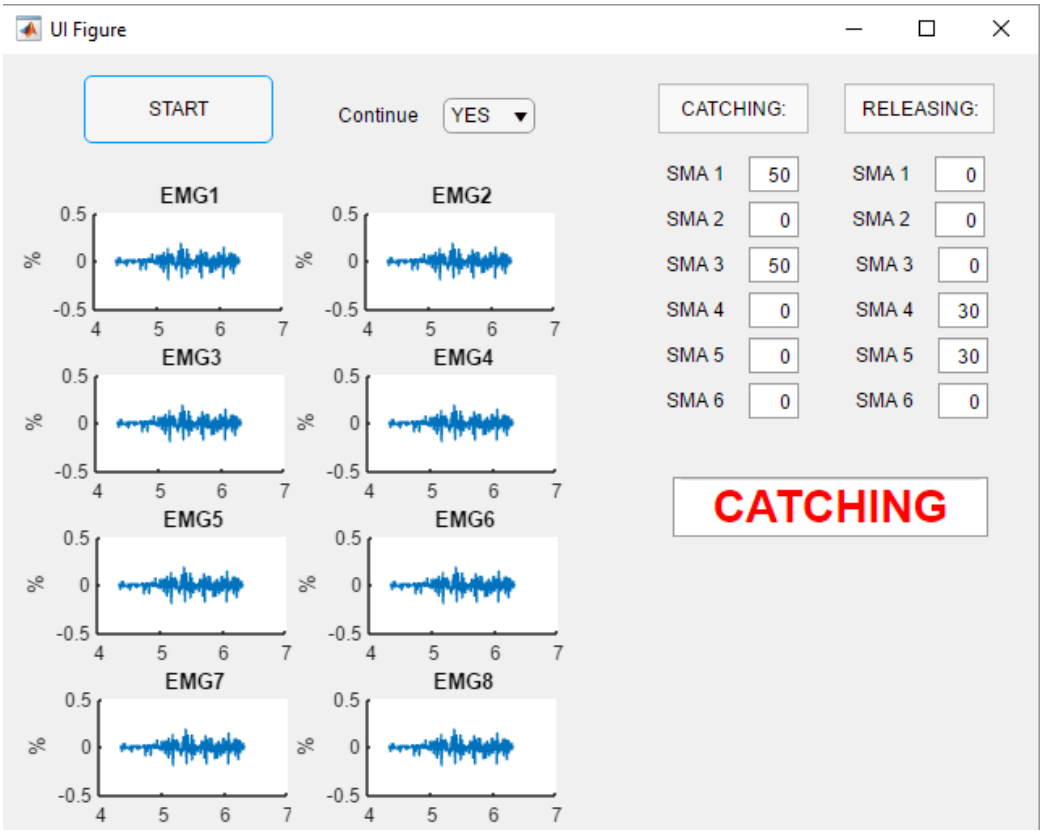

Figure 5.6 UI when the patient grasps the object

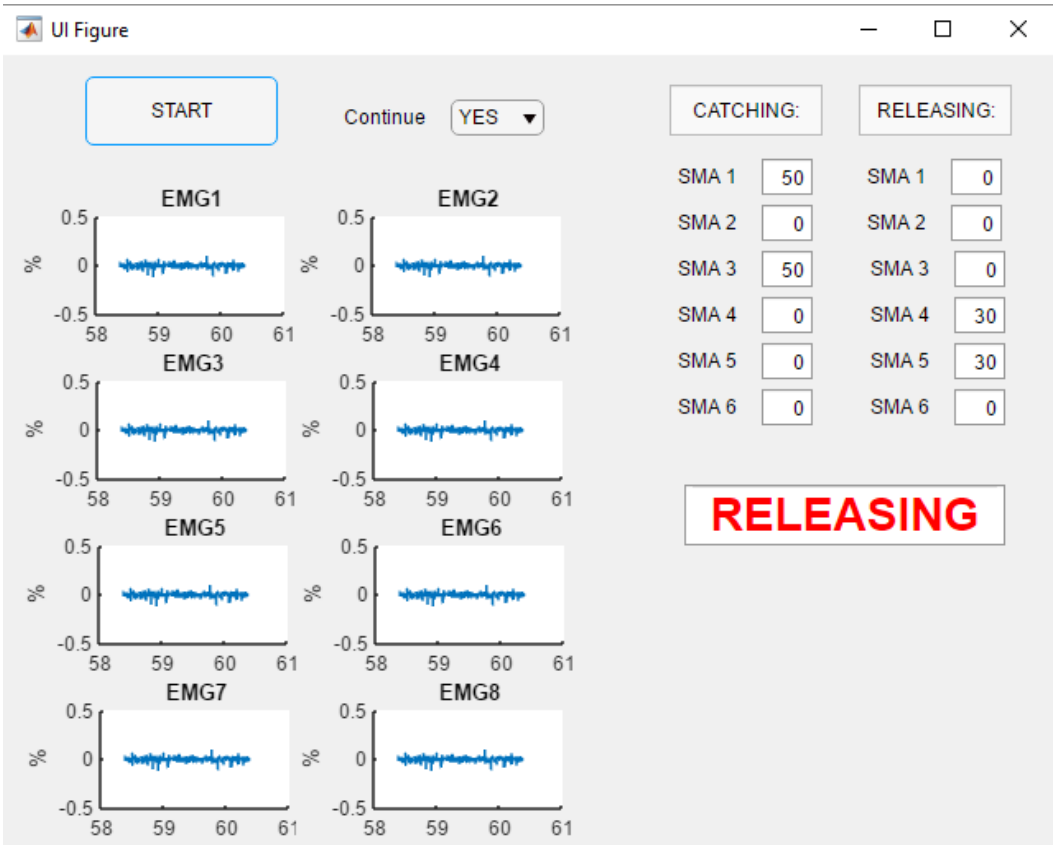

Figure 5.7 UI when the patient releases the object

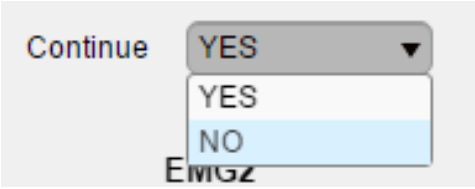

Figure 5.8 Drop down button

5.3. REAL-TIME RESULTS

The response time from when a person grasps or releases the object to when the actuators that move the exoskeletal hand were activated was measured ten times for each movement (TABLE 5.1).

TABLE 5.1 RESPONSE TIME FOR GRASPING (LEFT) AND RELEASING (RIGHT) IN SECONDS

RESPONSE TIME FOR GRASPING (IN SECONDS)	RESPONSE TIME FOR RELEASING (IN SECONDS)
0.68	1.05
1.19	1.66

1.03	2.10
0.96	1.79
1.09	2.72
1.21	1.53
0.80	2.15
1.13	1.96
0.32	2.53
0.52	1.35

The mean time delay from when a person is catching the object to when the actuators move is 0.893s. The mean time delay from when a person is releasing the object to when the actuators move is 1.884s.

The mean response time obtained for grasping is around the length of the window used to record the signal, which is one second. Therefore, the time delay is probably due to this window length and not to the SMA control system. As a result, if the window length is decreased, the time delay should decrease as well. Nevertheless, when testing the classifier with a smaller window length, of 0.5 s instead of 1 s, classification performance decreases to 95% in the case of catching and to 60% in the case of releasing, which is not acceptable.

The fact that the time delay for releasing is more than the window length implies that some signals are not being recognized as releasing until the subject has finished releasing the object and the hand is relaxed, whereas for catching, recognition is achieved at the beginning of the movement.

Decreasing the time delay without shortening the window length can be achieved by generating overlapped windows instead of adjacent ones when acquiring the signals. Instead of recording one signal every second, more signals can be recorded if the following signal does not start in the sample next to the last sample of the previous

recording but some number of samples before, as illustrated in the following diagram (Figure 5.9):

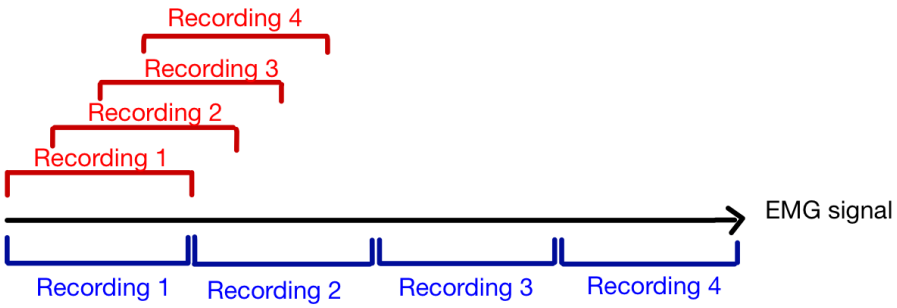

Figure 5.9 Adjacent acquisition system (blue) vs overlapping acquisition system (red)

Although theoretically this method seems promising for reducing the time delay, it can also increase the computational load by processing and classifying more signals than in the current approach. If too many signals are taken, the system could be slowed down. A compromise should be made in which the optimal number of signals with 1 s length are taken.

The control system was tested with the hand exoskeletons developed by Patricia Enríquez and Laura López in their Bachelor Thesis (Figure 5.10). The combination of this project with their devices was a success. The control system was able to detect when the subject grasps the object and the SMA actuators needed to hold the object were activated. The object was held until the hand of the subject was relaxed. When this relaxation was detected, the SMA actuators needed to open the hand were activated.

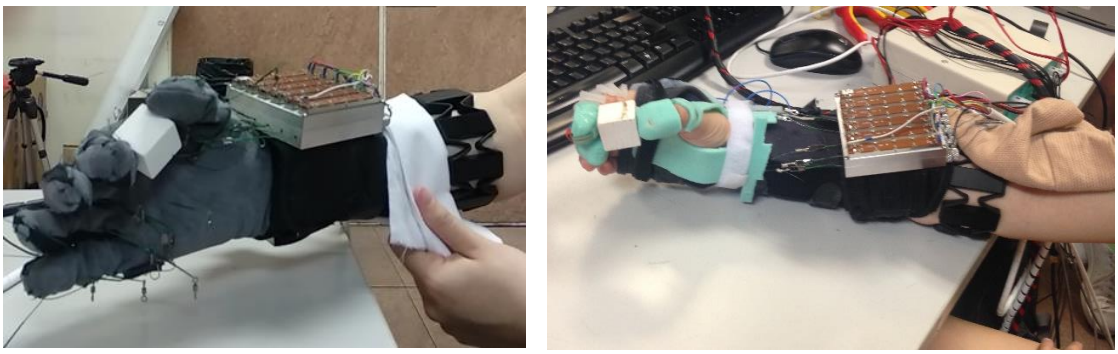

Figure 5.10 Trial with hand exoskeleton of Patricia Enríquez (left) and trial with hand exoskeleton of Laura López (right).

6. SOCIO-ECONOMIC ENVIRONMENT AND REGULATORY FRAMEWORK

6.1. SOCIO-ECONOMIC IMPACT

Hand injuries have a significant impact in the patient's work capacity, daily life activities and leisure activities, affecting negatively both individuals and society. These injuries constitute a high cost to society by increasing both healthcare costs, which arise from diagnostic procedures, operations and rehabilitation, and costs due to lost production[75]. Studies show that hand and wrist injuries represent the most expensive type of wounds, compared, for example, to knee and lower-limb fractures, skull-brain injuries, or hip fractures. This is mainly caused by the productivity costs [76]. For patients who have suffered stroke, rehabilitation is usually long-term, lasting months or years after stroke.

The World Health Organization (WHO) insists in the necessity to scale up rehabilitation [77]. The global need for rehabilitation is predicted to increase due to the rise of life expectancies and survival rates for those with severe disability. Furthermore, the prevalence of stroke has increased 21.8 % from 2005 to 2015 according to the WHO [77].

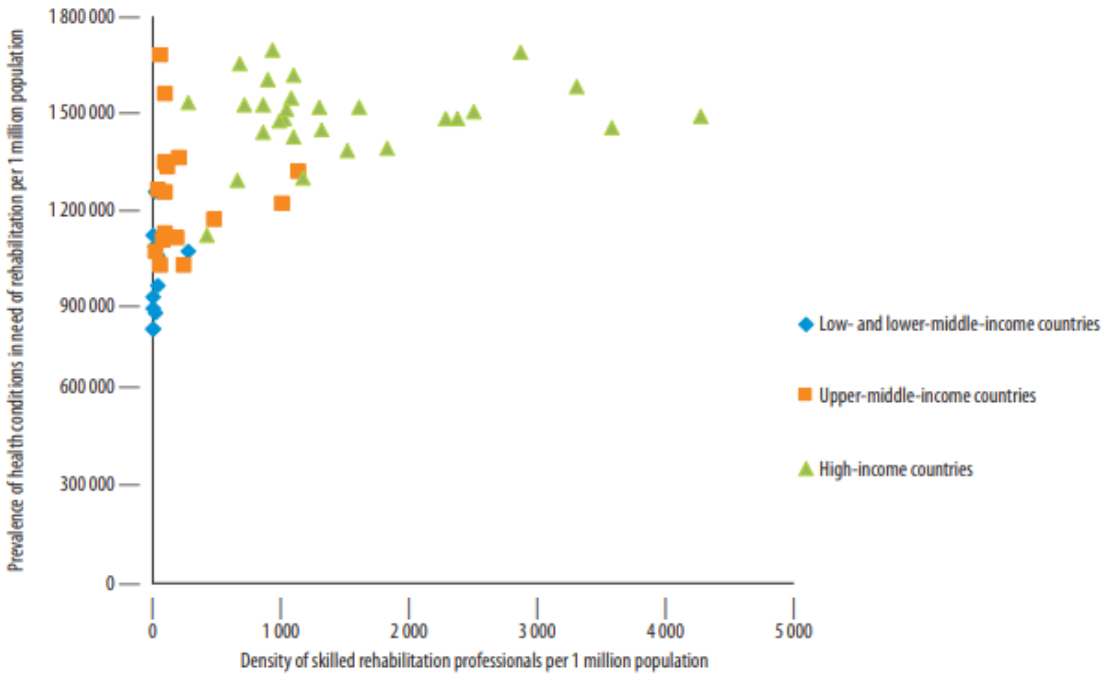

Figure 6.1 Prevalence of rehabilitation-relevant health conditions compared to the density of skilled rehabilitation professionals who can deliver. [77]

As can be seen in Figure 6.1, the density of skilled rehabilitation professionals is much lower than the need of rehabilitation, both in low and high income countries. The

capabilities of exoskeletons of producing repetitive and controllable motions make them desirable for replacing some of the functions of the rehabilitation therapists. These robotic systems will only succeed in their mission of substituting the therapist if they can function automatically. A reliable control system is essential for this purpose. These systems can save money and time, as the average hospital stay and the number of therapists needed per patient decreases. Exoskeletons can also increase the accessibility of rehabilitation, as they can be used for home rehabilitation and home care [78].

Training of users and carers must also be taken into account as a socio-economic impact, as they have to get used to these new devices and learn how to use them properly. To decrease the training time and effort, systems must be made as simple and easy to use as possible.

6.1. BACHELOR'S THESIS BUDGET

One of the greatest costs associated with this project is the Matlab and Simulink license. The code was developed with the Matlab's license from the UC3M. Nevertheless, if this project was developed by another entity, that entity must pay the license, which corresponds to 2000 euros. Another important cost comes from the use of the Myo Armband, which currently costs 199 USD, or 170 euros. The cost of the microcontroller must also be taken into account, as well as the cost of the computer for the time that it was used. The microcontroller's price is 17 euros. The laptop cost 1200 euros, and its average lifespan is 4 years [79]. The time required to develop this project was six months. Therefore, the cost associated with the laptop is: $\frac{lap_{price}}{12x4\ months} x6\ months = \frac{1200}{12x4} x6 = 150\ euros$.

Finally, the budget must also include the cost for the time invested in the project. It has required six months of part time work from the student and also time to think about the project and supervising it from the tutor, which corresponds to approximately 40 hours of work. The average student wage is 8 euros/hour, and the student has worked 360 hours. Therefore the cost for the time invested by the student is 2880 euros. The average professor wage is 15 euros/hour. Consequently, the cost of the time invested by the professor corresponds to 600 euros. The total cost of the working time is 3480 euros.

TABLE 6.1 BACHELOR'S THESIS BUDGET

ITEM	COST (EUROS)
Matlab and Simulink license	2000
Myo Armband	170
Microcontroller	17
Laptop	150
Working time	3480
TOTAL	5817

As TABLE 6.1 shows, the total budget required for this project is 5817 euros.

6.2. REGULATORY FRAMEWORK

The system is currently a prototype and has only been used with healthy subjects. The next step would be to test it with rehabilitation patients. This will require to stablish a protocol that must be validated by the ethical committee of the hospitals or rehabilitation centers where these trials are performed. If classification accuracy decreases when the system is used with patients, patient's data will be necessary to train the classifier. Data-protection laws must be considered when acquiring data from patients. In Spain, the Organic Law of Data Protection, Article 8, states the regulation of data relative to health [80]. According to this article, health professionals can use the data of their patients in accordance with the autonomic legislation. Nevertheless, health data can only be used under the express consent of the patient.

Once the system has been tested and is ready to be commercialized, it should be validated and comply with the medical equipment regulations and standards. These regulations vary from country to country. In Europe, the device requires European Conformity (CE) marking. To obtain the CE mark, safety and performance requirements must be fulfilled. There are three European directives regarding medical devices. The one that applies to this project is the Medical Devices Directive (93/42/EEC) [81]. This directive states that the devices must be designed and manufactured in such a way that, when used for the intended purpose, they will not compromise the clinical condition or the safety of patients,

or the safety and health of users, among other requirements. Europe has also regulations regarding the development of robots and artificial intelligence for medical use. In a European Parliament resolution from February 2017 [82], several recommendations were made regarding this issue. The resolution stresses the importance of a proper education and training for health professionals. Concerning rehabilitation robots specifically, the resolution notes that continuous access to maintenance, improvements and software updates should be guaranteed to the users of these devices. Finally, it highlights the importance of ensuring equal opportunities of accessing all these technological innovations to all individuals that need them. In order to commercialize the device in the United States, Food and Drug Administration (FDA) approval will be necessary.

Myo Armband is already a commercial device. Therefore, it already meets all requisites as it has obtained the CE marking.

Regarding the system's software, Matlab is necessary to run the system. Therefore, any institution willing to use the system must purchase a Matlab license. The patents from all algorithms used in this project for signal processing and classification are licensed by MathWorks Inc. through Matlab.

7. CONCLUSSIONS

The main objective of this thesis was to develop a real-time control system for light-weight, low-cost hand exoskeletons. The developed system is able to recognize two different motions using the patient's EMG signals. The EMG signal acquisition mechanism, the Myo Armband, is convenient, as it is non-invasive and it does not require previous preparation of the patient's skin in order to record the EMG signals. Furthermore, it can be easily placed in the forearm of the patient and it provides similar measurements in different sessions and with different patients. Another great advantage of this system is that it is wireless, as it communicates with the computer via Bluetooth. The neural network trained for movement classification is able to distinguish with higher accuracy the action of grasping than the action of releasing, probably due the way in which the training set was acquired.

After movement recognition, the system is able to communicate with a microcontroller that activates and deactivates the SMA wires used for grasping and releasing an object as soon as one of these movement is detected. All the process from when the patient moves his or her hand to when the exoskeletal hand is actuated occurs almost in real time, with a mean time delay of less than 1 second for the movement of grabbing an object and less than 2 seconds for the movement of releasing the object. This delay is acceptable, although it could be improved. Decreasing this response time should be the main objective of future improvements of this project, and it should be focused on decreasing the classification time, which is likely the cause of this delay.

The principal drawback of this control system is that it can only be used in patients with a certain level of motility, as they should start the movement before the robotic hand helps them.

7.1. FUTURE WORK

Several advances can be made to the project to make it more practical for clinical use. The system may increase classification accuracy if parameters from the neural network, such as the number of hidden layers, or the training and performance algorithms are optimized. Classification accuracy with patients should also be tested because their EMG signals may differ from the ones used to train the classifier, which were taken from a healthy person. If the accuracy decreases under acceptable limits, training the classifier with data taken from the patients should be considered.

Although the hand exoskeletons that are being currently developed in the Robotics Lab of the UC3M have been designed to help rehabilitation patients with the opening and closing of the hand and of different fingers separately, the advantage of having used machine learning in this project is that many other movements can be detected with this method, as Irene Mendez demonstrated [39]. A system able to recognize movements such as pronation or supination of the hand as well as opening and closing it can be used to control hand exoskeletons able to help with these tasks.

Another interesting improvement that can be implemented and that was not performed in this project due to time constrains is to integrate the system with a computer serious game, which is a game developed not only for entertainment. In this case, the game would try to imitate exercises included on traditional physical therapy. This tool can increase the motivation of rehabilitation patients by distracting the patients from the fact that they are in a rehabilitation session. A series of serious games have already been developed in the Robotics Lab of the UC3M [83]. The ones that require the patient to grasp an object, perform some task, and release the object, can be directly integrated with the system developed in this project.

In order to decrease the price of the system, an open-source programming language, such as Python, can be used instead of Matlab, which requires a costly license. The use of a computer can also be avoided if all the code is integrated into the microcontroller. This would eliminate the time needed to write data from the computer into the microcontroller, making the control system even faster.

To conclude, this project has demonstrated that the technology developed by Thalamic Labs, the Myo Armband, combined with machine learning, constitutes a powerful tool to control hand exoskeletons in real time. This opens up a lot of opportunities for controlling robotic systems with the movement of someone's hand, which could greatly benefit rehabilitation therapies, allowing for activities where the patient not only performs repetitive movements, but also decides when to perform these movements, focusing more on active therapies than on passive ones.

8. BIBLIOGRAPHY

[1] by Zheng Li and J. F. Muth Ola L A Harrysson, “USING ROBOTIC HAND TECHNOLOGY FOR THE REHABILITATION OF RECOVERING STROKE PATIENTS WITH LOSS OF HAND POWER,” 2003.

[2] L. W. Pedretti, H. M. Pendleton, and W. Schultz-Krohn, *Pedretti’s occupational therapy : practice skills for physical dysfunction*. Elsevier, 2013.

[3] G. Yavuzer *et al.*, “Mirror Therapy Improves Hand Function in Subacute Stroke: A Randomized Controlled Trial,” *Arch. Phys. Med. Rehabil.*, vol. 89, no. 3, pp. 393–398, Mar. 2008.

[4] P. Enríquez, “Soft hand exoskeleton with SMA actuation of each finger separately,” Bachelor Thesis, Universidad Carlos III de Madrid, 2018.

[5] L. López, “Soft hand exoskeleton actuated with SMA fibers,” Bachelor Thesis Universidad Carlos III de Madrid, 2018.

[6] “Rehabilitation for Neurological Disorders | Johns Hopkins Medicine Health Library.” [Online]. Available: https://www.hopkinsmedicine.org/healthlibrary/conditions/nervous_system_disorders/rehabilitation_for_neurological_disorders_85,P00801. [Accessed: 20-Apr-2018].

[7] “Movement Disorders - neurosymptoms.org.” [Online]. Available: http://www.neurosymptoms.org/movement-disorders/4533053142. [Accessed: 20-Apr-2018].

[8] C. H. Polman *et al.*, “Diagnostic criteria for multiple sclerosis: 2010 Revisions to the McDonald criteria,” *Ann. Neurol.*, vol. 69, no. 2, pp. 292–302, Feb. 2011.

[9] “Active vs Passive Exercises during Rehab – Flint Rehab.” [Online]. Available: https://www.flintrehab.com/2015/active-vs-passive-exercises-during-rehab/. [Accessed: 20-Apr-2018].

[10] “Post-Stroke Rehabilitation Fact Sheet | National Institute of Neurological Disorders and Stroke.” [Online]. Available: https://www.ninds.nih.gov/Disorders/Patient-Caregiver-Education/Fact-Sheets/Post-Stroke-Rehabilitation-Fact-Sheet. [Accessed: 20-Apr-2018].

[11] T. Rose, C. S. Nam, and K. B. Chen, “Immersion of virtual reality for rehabilitation - Review,” *Appl. Ergon.*, vol. 69, no. February 2017, pp. 153–161, 2018.

[12] D. A. T. Soupikova *et al.*, “Virtual Immersion for Post-Stroke Hand Rehabilitation Therapy,” vol. 43, no. 2, pp. 467–477, 2015.

[13] Physiopedia contributions, “Mirror Therapy,” *Physiopedia*, 2018. .

[14] P. Heo, G. M. Gu, S. jin Lee, K. Rhee, and J. Kim, “Current hand exoskeleton technologies for rehabilitation and assistive engineering,” *Int. J. Precis. Eng. Manuf.*, vol. 13, no. 5, pp. 807–824, 2012.

[15] P. Maciejasz, J. Eschweiler, K. Gerlach-Hahn, A. Jansen-Troy, and S. Leonhardt, “A survey on robotic devices for upper limb rehabilitation,” *J. Neuroeng. Rehabil.*, vol. 11, no. 1, pp. 1–29, 2014.

[16] P. Poli, G. Morone, G. Rosati, and S. Masiero, “Robotic technologies and rehabilitation: New tools for stroke patients’ therapy,” *Biomed Res. Int.*, vol. 2013, 2013.

[17] C. N. Schabowsky, S. B. Godfrey, R. J. Holley, and P. S. Lum, “Development and pilot testing of HEXORR: Hand exoskeleton rehabilitation robot,” *J. Neuroeng. Rehabil.*, vol. 7, no. 1, pp. 1–16, 2010.

[18] L. Dovat *et al.*, “HandCARE: A cable-actuated rehabilitation system to train hand function after stroke,” *IEEE Trans. Neural Syst. Rehabil. Eng.*, vol. 16, no. 6, pp. 582–591, 2008.

[19] M. Bouzit, G. Popescu, G. Burdea, and R. Boian, “The Rutgers Master II-ND force feedback glove,” *Proc. - 10th Symp. Haptic Interfaces Virtual Environ. Teleoperator Syst. HAPTICS 2002*, no. February, pp. 145–152, 2002.

[20] O. Lambercy, L. Dovat, R. Gassert, E. Burdet, C. L. Teo, and T. Milner, “A haptic knob for rehabilitation of hand function,” *IEEE Trans. Neural Syst. Rehabil. Eng.*, vol. 15, no. 1, pp. 356–366, 2007.

[21] “InMotion HAND™ - Bionik Labs.” [Online]. Available: http://bionikusa.com/healthcarereform/upper-extremity-rehabilitiation/inmotion-hand/. [Accessed: 08-May-2018].

[22] “Hand Mentor Pro™ - Motus Nova | Your Partner for Improving Mobility.” [Online]. Available: https://motusnova.com/products/hand-mentor-pro/. [Accessed: 08-May-2018].

[23] T. G. Sugar *et al.*, “Design and control of RUPERT: A device for robotic upper extremity repetitive therapy,” *IEEE Trans. Neural Syst. Rehabil. Eng.*, vol. 15, no. 1, pp. 336–346, 2007.

[24] C. D. Takahashi, L. Der-Yeghiaian, V. Le, R. R. Motiwala, and S. C. Cramer, “Robot-based hand motor therapy after stroke,” *Brain*, vol. 131, no. 2, pp. 425–437, 2008.

[25] E. B. Brokaw, I. Black, R. J. Holley, and P. S. Lum, “Hand Spring Operated Movement Enhancer (HandSOME): A portable, passive hand Exoskeleton for stroke rehabilitation,” *IEEE Trans. Neural Syst. Rehabil. Eng.*, vol. 19, no. 4, pp. 391–399, 2011.

[26] “Bioness Inc. - H200 for Hand Paralysis.” [Online]. Available: https://www.bioness.com/Products/H200_for_Hand_Paralysis.php. [Accessed: 08-May-2018].

[27] “About Us.” [Online]. Available: http://www.exoslim.tuiasi.ro/. [Accessed: 08-May-2018].

[28] S. Pittaccio and S. Viscuso, “Shape Memory Actuators for Medical Rehabilitation and Neuroscience,” *Smart Actuation Sens. Syst. - Recent Adv. Futur. Challenges*, 2012.

[29] “AMADEO.” [Online]. Available: http://tyromotion.com/en/products/amadeo. [Accessed: 08-May-2018].

[30] F. J. Badesa, A. Blanco, N. Garcı, and L. D. Lledo, “Hand exoskeleton for rehabilitation therapies with integrated optical force sensor,” vol. 10, no. 2, pp. 1–11, 2018.

[31] C. Fleischer, A. Wege, K. Kondak, and G. Hommel, “Application of EMG signals for controlling exoskeleton robots,” *Biomed. Tech.*, vol. 51, no. 5–6, pp. 314–319, 2006.

[32] M. Mulas, M. Folgheraiter, and G. Gini, “An EMG-controlled exoskeleton for hand rehabilitation,” in *Proceedings of the 2005 IEEE 9th International Conference on Rehabilitation Robotics*, 2005, vol. 2005, pp. 371–374.

[33] K. Y. Tong *et al.*, “An intention driven hand functions task training robotic system,” in *2010 Annual International Conference of the IEEE Engineering in Medicine and Biology Society, EMBC’10*, 2010, pp. 3406–3409.

[34] Y. Hasegawa, Y. Mikami, K. Watanabe, and Y. Sankai, “Five-fingered assistive hand with mechanical compliance of human finger,” in *Proceedings - IEEE International Conference on Robotics and Automation*, 2008, pp. 718–724.

[35] H. In and C. KyuJin, “Compact Hand Exoskeleton Robot for the Disabled,” in *The 6th International Conference on Ubiquitous Robots and Ambient Intelligence (URAI 2009)*, 2009, no. Urai, pp. 1–4.

[36] M. Dicicco, L. Lucas, Y. Matsuoka, and M. Engineering, “Comparison of Control Strategies for an EMG Controlled Orthotic Exoskeleton for the Hand,” *Int. Conf. Robot. Autom.*, no. April, pp. 1622–1627, 2004.

[37] N. Benjuya and S. B. Kenney, “Myoelectric Hand Orthosis,” *JPO Journal of Prosthetics & Orthotics*, vol. 2. pp. 149–154, 1990.

[38] B. Karlık, “Machine Learning Algorithms for Characterization of EMG Signals,” *Int. J. Inf. Electron. Eng.*, vol. 4, no. 3, 2014.

[39] I. Méndez, “Implementation of a neural network-based electromyographic control system for a printed robotic hand,” Bachelor Thesis, Universidad Carlos III de

Madrid, 2016.

[40] A. Sánchez, “Matriz de electrodos EMG para detección de intención de movimiento de la mano,” Bachelor Thesis, Universidad Carlos III de Madrid, 2017.

[41] “Gesture Control Armband using Single EMG and IMU sensor – Cuong’s Blog.” [Online]. Available: http://cuongtv.com/project/Gesture-Control-Armband-using-Single-EMG-and-IMU-sensor/. [Accessed: 26-May-2018].

[42] “electromyography | Definition of electromyography in English by Oxford Dictionaries.” [Online]. Available: https://en.oxforddictionaries.com/definition/electromyography. [Accessed: 26-May-2018].

[43] Silverthorn, *Human Physiology An Integrated Approach*. .

[44] “The Autonomic Nervous System.” [Online]. Available: https://antranik.org/the-autonomic-nervous-system/. [Accessed: 26-May-2018].

[45] “Synap-tic Trans-mis-sion at the Neu-ro-mus-cu-lar... - Nervous System - Neuroanatomy.” [Online]. Available: http://neuroanatomyblog.tumblr.com/post/22862465112/synap-tic-trans-mis-sion-at-the-neu-ro-mus-cu-lar. [Accessed: 26-May-2018].

[46] P. M. Hopkins, “Skeletal muscle physiology,” *Contin. Educ. Anaesthesia, Crit. Care Pain*, vol. 6, no. 1, pp. 1–6, 2006.

[47] “Motor unit action potentials | definition of Motor unit action potentials by Medical dictionary.” [Online]. Available: https://medical-dictionary.thefreedictionary.com/Motor+unit+action+potentials. [Accessed: 26-May-2018].

[48] “Motor Unit Presentation.” [Online]. Available: http://163.178.103.176/Fisiologia/general/activ_bas_3/MotorUnit.htm. [Accessed: 26-May-2018].

[49] “Tech Specs | Myo Battery Life, Dimensions, Compatibility, and More.” [Online]. Available: https://www.myo.com/techspecs. [Accessed: 26-May-2018].

[50] “Myo SDK 0.9.0: Getting Started.” [Online]. Available: https://developer.thalmic.com/docs/api_reference/platform/getting-started.html. [Accessed: 27-May-2018].

[51] S. N. Sidek and A. J. H. Mohideen, “Measurement system to study the relationship between forearm EMG signals and wrist position at varied hand grip force,” *2012 Int. Conf. Biomed. Eng. ICoBE 2012*, no. February, pp. 169–174, 2012.

[52] “Muscles of the Shoulder. Muscles of the Arm. Muscles of the Forearm.” [Online]. Available: http://encyclopedia.lubopitko-bg.com/Muscles_of_the_Shoulder.html. [Accessed: 26-May-2018].

[53] “Myo SDK 0.9.0: Myo SDK Manual.” [Online]. Available: https://developer.thalmic.com/docs/api_reference/platform/index.html. [Accessed: 27-May-2018].

[54] “Using the Myo Bluetooth adapter – Welcome to Myo Support.” [Online]. Available: https://support.getmyo.com/hc/en-us/articles/201105145-Using-the-Myo-Bluetooth-adapter. [Accessed: 27-May-2018].

[55] “Getting starting with Myo on Windows – Welcome to Myo Support.” [Online]. Available: https://support.getmyo.com/hc/en-us/articles/202657596. [Accessed: 27-May-2018].

[56] “Myo SDK MATLAB MEX Wrapper - File Exchange - MATLAB Central.” [Online]. Available: https://es.mathworks.com/matlabcentral/fileexchange/55817-myo-sdk-matlab-mex-wrapper. [Accessed: 27-May-2018].

[57] M. a. Oskoei and H. H. H. Hu, “Support Vector Machine-Based Classification Scheme for Myoelectric Control Applied to Upper Limb,” *IEEE Trans. Biomed. Eng.*, vol. 55, no. 8, pp. 1956–1965, 2008.

[58] J. Valls-Solé, J. C. Rothwell, F. Goulart, G. Cossu, and E. Muñoz, “Patterned ballistic movements triggered by a startle in healthy humans,” *J. Physiol.*, vol. 516, no. 3, pp. 931–938, 1999.

[59] C. I. Christodoulou and C. S. Pattichis, “Unsupervided pattern recognition for the classification of EMG signals,” *IEEE Trans. Biomed. Eng.*, vol. 46, no. 2, pp. 169–178, 1999.

[60] M. Zecca, S. Micera, M. C. Carrozza, and P. Dario, “Control of Multifunctional Prosthetic Hands by Processing the Electromyographic Signal,” *Crit. Rev. Biomed. Eng.*, vol. 30, no. 4–6, pp. 459–485, 2002.

[61] E. J. Rechy-Ramirez and H. Hu, “Stages for Developing Control Systems using EMG and EEG Signals: A survey,” 2011.

[62] R. C. Gonzalez and R. E. Woods, *Digital Image Processing*, vol. 49. 2008.

[63] K. Englehart, B. Hudgins, P. A. Parker, and M. Stevenson, “Classification of the myoelectric signal using time-frequency based representations,” *Med. Eng. Phys.*, vol. 21, no. 6–7, pp. 431–438, 1999.

[64] A. Tharwat, T. Gaber, A. Ibrahim, and A. E. Hassanien, “Linear discriminant analysis: A detailed tutorial,” *AI Commun.*, vol. 30, no. 2, pp. 169–190, 2017.

[65] L. J. Williams, “Principal Component Analysis,” *English*, vol. 2, no. 4, pp. 433–470, 2010.

[66] “Principal component analysis of raw data - MATLAB pca - MathWorks España.” [Online]. Available: https://es.mathworks.com/help/stats/pca.html. [Accessed: 28-May-2018].

[67] A. Abraham, “Neural Networks,” 2005.

[68] M. A. Nanda, K. B. Seminar, D. Nandika, and A. Maddu, “A comparison study of kernel functions in the support vector machine and its application for termite detection,” *Inf.*, vol. 9, no. 1, 2018.

[69] P. Cunningham and S. J. Delany, “K -Nearest Neighbour Classifiers,” *Tech. Rep. UCD-CSI-2007-4*, no. May 2014, pp. 1–17, 2007.

[70] J. M. Keller and M. R. Gray, “A Fuzzy K-Nearest Neighbor Algorithm,” *IEEE Trans. Syst. Man Cybern.*, vol. SMC-15, no. 4, pp. 580–585, 1985.

[71] A. P. Bradley, “The Use of the Area Under the ROC Curve in the Evaluation of Machine Learning Algorithms,” pp. 1–33.

[72] “Confusion matrix - mlxtend.” [Online]. Available: https://rasbt.github.io/mlxtend/user_guide/evaluate/confusion_matrix/. [Accessed: 29-May-2018].

[73] D. Copaci, A. Flores, F. Rueda, I. Alguacil, D. Blanco, and L. Moreno, “Wearable Elbow Exoskeleton Actuated with Shape Memory Alloy,” Springer, Cham, 2017, pp. 477–481.

[74] J. M. Esposito and U. S. N. Academy, “Tutorial : Serial Communication in Matlab,” pp. 1–16, 2009.

[75] H.-E. Rosberg, K. S. Carlsson, R. I. Cederlund, E. Ramel, and L. B. Dahlin, “Costs and outcome for serious hand and arm injuries during the first year after trauma – a prospective study,” *BMC Public Health*, vol. 13, p. 1, 2013.

[76] “The Cost of Hand and Wrist Injuries | EHS Today.” [Online]. Available: http://www.ehstoday.com/health/cost-hand-and-wrist-injuries. [Accessed: 30-May-2018].

[77] “The need to scale up rehabilitation.”

[78] E. Mikołajewska and D. Mikołajewski, “Exoskeletons in Neurological Diseases – Current and Potential Future Applications Egzoszkielety w terapii schorzeń neurologicznych – zastosowania obecne i przyszłe,” 2013.

[79] A. Hoang, W. Tseng, S. Viswanathan, and H. Evans, “Life Cycle Assessment of a Laptop Computer and its Contribution to Greenhouse Gas Emissions,” no. February, pp. 1–8, 2012.

[80] “Ley Orgánica 15/1999, de 13 de diciembre, de Protección de Datos de Carácter Personal. TÍTULO II. Principios de la protección de datos.” [Online]. Available: http://noticias.juridicas.com/base_datos/Admin/lo15-1999.t2.html#a8. [Accessed: 10-Jun-2018].

[81] “EUR-Lex - 31993L0042 - EN - EUR-Lex.” [Online]. Available: https://eur-lex.europa.eu/legal-content/EN/TXT/?uri=CELEX:31993L0042. [Accessed: 13-

Jun-2018].

[82] “Textos aprobados - Jueves 16 de febrero de 2017 - Normas de Derecho civil sobre robótica - P8_TA(2017)0051.” [Online]. Available: http://www.europarl.europa.eu/sides/getDoc.do?pubRef=-//EP//TEXT+TA+P8-TA-2017-0051+0+DOC+XML+V0//ES. [Accessed: 13-Jun-2018].

[83] R. C. la C. S. C.-V. C. B. E. Oña A. Jardon, “Effectiveness of Serious Games for Leap Motion on the Functionality of the Upper Limb in Parkinson’s Disease: A Feasibility Study,” *Comput. Intell. Neurosci.*, vol. 2018, p. , 2018.